

On the Accuracy of Marine Gravity Measurements

PÁL WESSEL AND ANTHONY B. WATTS

*Lamont-Doherty Geological Observatory and Department of Geological Sciences, Columbia University
Palisades, New York*

We have assessed the accuracy of Lamont-Doherty Geological Observatory's global marine gravity data bank by examining the crossover errors (COEs) at intersecting ship tracks. More than 63,000 COEs were found, having a standard deviation of 22.43 mGal (mGal = 10^{-5} m s⁻²). We use the COEs to find and remove linear drifts and DC shifts present in the data set. This adjustment reduces the standard deviation to 13.96 mGal. COEs generally decrease with latitude, which we attribute to uncertainties in the Eötvös correction. High COEs occur in areas of high gravity gradients. These two features point to poor navigation as the principal source of error in marine gravity surveys. COEs have generally been decreasing during the last two decades, reflecting improvements in instrumentation and quality of navigation. A comparison of the shipboard gravity data to Seasat derived gravity revealed a 9-mGal bias in the terrestrial data, which probably reflects uncertainties in choice of reference field. The adjusted data set was used to generate a gravimetric geoid for the NW Atlantic Ocean. By removing this geoid from the Seasat sea surface heights, a residual "geoid" was obtained. A special feature of this map is an elongate ENE trend that appears to correlate with the edge of the Gulf Stream.

INTRODUCTION

During the past few decades there have been numerous gravity measurements obtained over the Earth's surface by university, government, and industry groups. The global data bank at the Lamont-Doherty Geological Observatory (LDGO) currently contains more than 4.8 million point gravity measurements. This data set provides one of the principal means of determining crustal and upper mantle structure beneath oceans and continents. Its use in gravity model improvement, ground truth for satellite and airborne data, and gravimetric geoid computation has been somewhat limited, however, chiefly because of uncertainties in the accuracy of the data, particularly in the case of measurements obtained at sea [e.g. *Neuman and Talwani, 1972*].

In recent years a number of geologic, geodetic, and geophysical applications have stressed the need for a self-consistent globally adjusted gravity data set based on terrestrial measurements. For example, in gravity model improvement studies, terrestrial data are now being incorporated into combination solutions for the gravity field which are complete to degree and order 180. Although mean "block" gravity anomalies are now available over most of the Earth's surface [e.g., *Rapp, 1981*], there has been no systematic analysis of the accuracy of the point data used to construct these block anomaly means. In the case of most land data, errors due to instruments, drift, and topographic corrections are generally small and less than about 1 mGal. Marine data, on the other hand, can be subject to errors up to a few tens of mGal.

A major factor in the accuracy of marine gravity data is the quality of the ship's navigation. A primary error source is incorrect computation of the Eötvös effect, which is a strong function of the ship's heading and over-the-ground velocity. In order to achieve a 1-mGal accuracy for a ship traveling at

5 m s⁻¹ at the equator, for example, it is necessary to know the heading to better than 1° and the velocity to better than 0.1 m s⁻¹. Prior to about 1967, most ships utilized celestial navigation, so large errors (up to a few tens of mGal) may still remain in these data. The magnitude of the errors was thought to have been reduced following introduction of the U.S. Navy satellite navigation system (TRANSIT). However, it is generally agreed that significant errors related to navigational uncertainties still remain in gravity data, even those data acquired after 1967.

In addition to errors related to navigation, there are several other sources of error that contribute to uncertainties in marine gravity data. Among the most significant of these for measurements obtained with the beam-type sea gravimeters [*LaCoste, 1959; Graf and Schulze, 1961*] are off-leveling, cross-coupling, nonlinear drift and a mechanical "tare" or "jar" of the gravity measuring system.

Unfortunately, it is difficult to quantify the accuracy of marine gravity data because the types of navigation, measuring system response, and sea conditions vary among individual legs. The principal method used to estimate the accuracy of gravity data at sea has been the analysis of the discrepancies in free-air gravity anomaly values at intersecting ship tracks [e.g., *Talwani, 1971*]. We believe this method to be the most reliable technique with which to evaluate the accuracy of marine gravity data. Most previous studies have computed the crossover discrepancies manually and so have only assessed the accuracy of gravity data over small regions of the ocean basins. This paper presents the results of a systematic analysis of the LDGO marine gravity data bank based on 63,257 ship track intersections. We have used gravity data collected along more than 3.7 million km of ship track by 16 different collecting agencies. The overall objectives of the study are (1) to provide statistical information on the accuracy of individual ship gravity surveys, (2) to determine the principal sources of error in gravity measurements at sea and, where possible, correct for these errors, and (3) to construct an "adjusted" gravity data base from which gridded averages can easily be computed and used in geologic, geodetic, and geophysical applications.

Copyright 1988 by the American Geophysical Union.

Paper number 7B1039.
0148-0227/88/007B-1039\$05.00

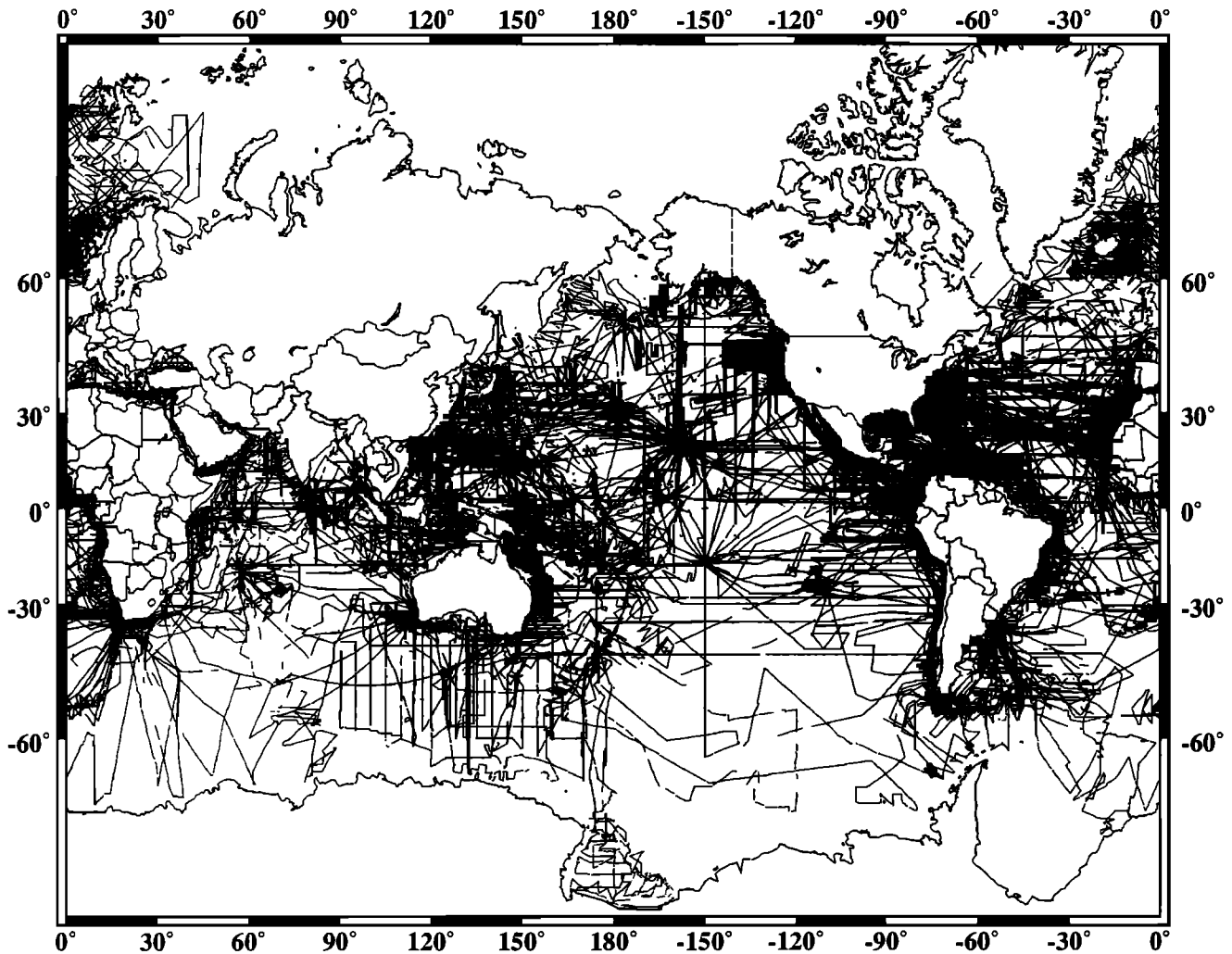


Fig. 1. Marine gravity measurements obtained by LDGO-operated research vessels (R/V *Vema*, R/V *Conrad*, and USNS *Ellanin*) and by other agencies since 1959.

GLOBAL GRAVITY DATA BASE

The gravity data bank at Lamont-Doherty is one of the largest libraries of unclassified terrestrial gravity measurements in the world. The bank contains only measured "point" anomaly values. In order to rapidly retrieve point gravity data we developed a system based on the concept of "bins" [e.g., *Karner and Watts*, 1983]. This system permits efficient storage and allows manipulation of large amounts of gravity data. Any measured value belongs to one geographical bin, and each bin can be accessed uniquely. In addition to observed gravity, the geodetic position, time of measurement, free-air gravity anomaly, elevation, Bouguer anomaly, and various source information are stored.

At present, approximately 2.6 million marine and 2.2 million land gravity point values have been binned [*Watts et al.*, 1985]. The distribution of the marine data is illustrated in Figure 1. While portions of the oceans have been intensely surveyed (e.g., central North Atlantic), there are large regions of sparse coverage, particularly south of 30° south. Figure 2 shows the principal collecting agencies for the marine data set. As can be seen from the figure, LDGO

has collected by far the largest amount of data of any agency. Together with data obtained by the National Oceanic and Atmospheric Administration, Woods Hole Oceanographic Institution, U.S. Navy, and Hawaii Institute of Geophysics, these data sets make up nearly 80% of the data base. Figure 3 shows that a majority of the marine measurements were acquired during the early 1970s. Gravity data acquisition increased slowly following the introduction of the first continuously recording sea gravity meter systems in 1960 and peaked about 1972. Since 1972, there has been a steady decline in the number of gravity measurements acquired annually.

GLOBAL GRAVITY CROSSOVER ANALYSIS

To assess the quality of marine gravity data, we need some measure of the accuracy and internal precision of individual cruises. The best approach to this problem is to determine the discrepancies in free-air gravity anomaly at intersecting ship tracks. Figure 4 defines the crossover error (COE) at the crossover point. We have developed a computer technique that, given a number of individual ship legs, computes COE values at all possible intersections between these legs.

Relative Contributions to Data Bank

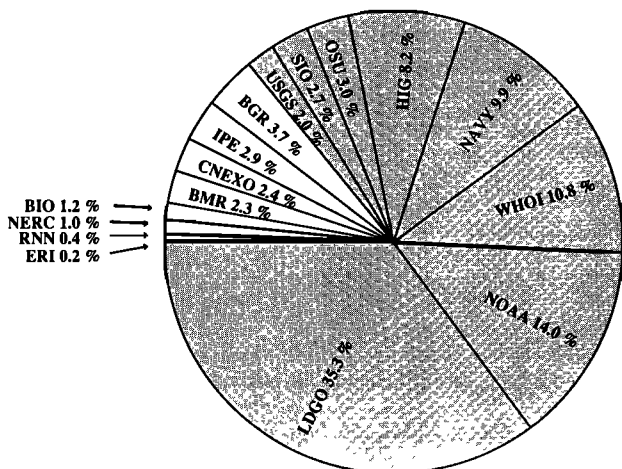


Fig. 2. Relative contribution to the data base by the 16 agencies involved. U.S. agencies (shaded) have collected ~85% of the data. Key: LDGO, Lamont-Doherty Geological Observatory; NOAA, National Oceanographic and Atmospheric Administration; WHOI, Woods Hole Oceanographic Institution; NAVY, U.S. Navy; HIG, Hawaii Institute of Geophysics; BGR, Bundesanstalt für Geowissenschaften und Rohstoffe (Germany); IPE, Institute Physics of the Earth (USSR); OSU, Oregon State University; SIO, Scripps Institute of Oceanography; BMR, Bureau of Mineral Resources (Australia); CNEXO, Centre National Pour L'Exploitation de Oceans (France); USGS, U.S. Geological Survey; BIO, Bedford Institute of Oceanography (Canada); NERC, Natural Environment Research Council (United Kingdom); RNN, Royal Netherlands Navy; and ERI, Earth Research Institute (Japan).

Several schemes of interpolation were tested (natural cubic spline, quasi-hermite spline [Akima, 1972] and linear interpolant) to compute gravity at the crossover point, and they all produced similar results (within ± 0.1 mGal). We used the linear interpolant, since it gave the lowest rms and required less processing time. In addition, the linear interpolant does not introduce undesirable oscillations near outliers or rapid change in gravity, as is the case with cubic splines. However, the cubic spline interpolant revealed that several of the legs contained single, erratic data points. Thus before the

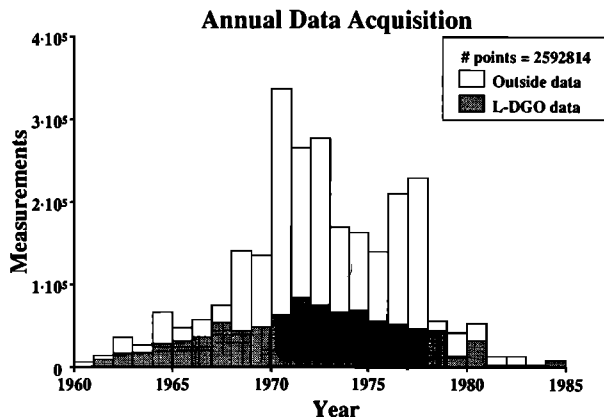


Fig. 3. Number of marine gravity measurements collected annually since 1959. Shaded portion of the data has been collected by LDGO-operated vessels. Close to 2.6 million data points have been acquired since the introduction of shipboard gravity meters.

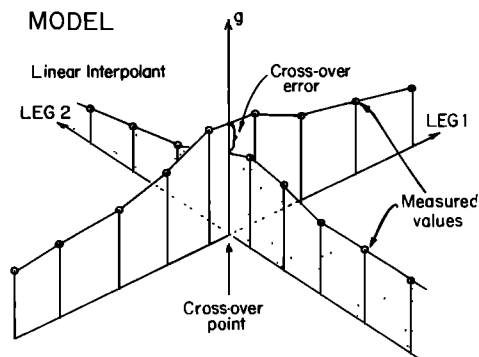


Fig. 4. Model for a crossover between two track segments. The crossover point is found by searching the navigation files. The discrepancy in free-air anomaly is computed by linear interpolation between the four points around the crossover point. If the time difference between the two points along any of the two tracks exceeded 15 min, a data gap was assumed, and no COE was computed.

COE analysis, we ran all the legs through a "despiking" filter. More than 75% of the legs had outliers that had to be removed.

Ideally there should be no COE, since we are measuring gravity at the "same" point, determined by our navigation. In general, this is not the case. For several reasons, the error may range from zero to several tens of mGals, and occasionally exceed 100 mGal. The possible sources of error are summarized in Table 1. When computing COEs, we made a distinction between "internal" and "external" COEs. The reason for this should be clear from Table 1. Internal COEs arise when a ship track crosses itself one or more times during a cruise leg, whereas external COEs involve two different ships' tracks. Since internal COEs have many parameters in common (e.g., same ship, sensor, quality of navigation, sea state), we expect that these errors on the average will be smaller than the external COEs, which often are produced by ships separated in time by a number of years and having different instrument sensitivity and navigation quality. Histograms showing the frequency distribution of both internal and external COEs are presented in Figure 5. The total number of internal and external COEs are 18,320 and 44,937, respectively, and represent all COEs generated by 834 legs in the global data set. Whereas the internal COEs have a standard deviation of 11.29 mGal, the standard

TABLE 1. Principal Sources of Error in Marine Gravity Surveys

Source	Errors
Instrument	Dynamic sensitivity of sensor Cross-coupling (Spring-type gravimeters) Off-leveling Mechanical "Tares" of suspension constraining mass displacement Nonlinear drift
Navigation	Incorrect Eötvös correction Incorrect positioning
Other	Incorrect tie-in to base stations Inconsistent use of reference field

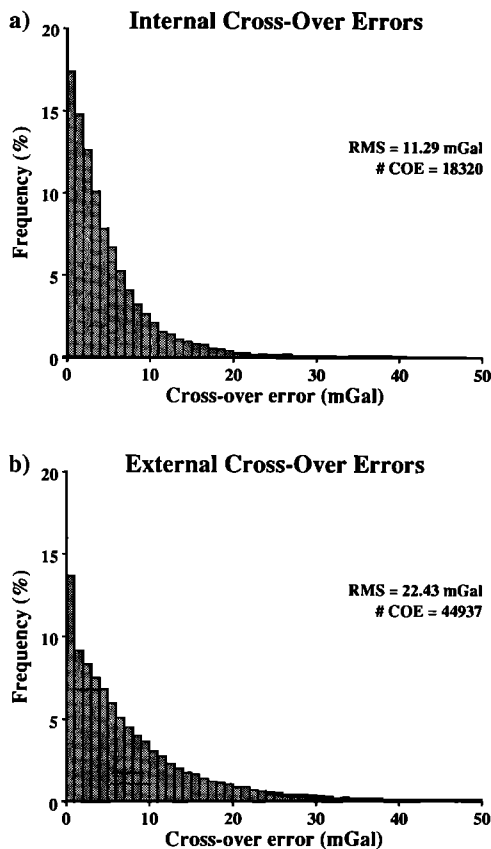


Fig. 5. (a) Histogram of the internal crossover errors for all legs before adjustments (only 610 legs had internal crossovers). Histogram interval is 1 mGal. Here 18,320 internal COEs have been found with an rms value of 11.29 mGal. (b) Histogram of the external crossover errors, same histogram interval. Here 44,937 external COEs have been generated from intersections among 822 legs. Of the 865 legs tested, 834 had crossovers (internal and/or external).

deviation of the external COEs is much larger (22.43 mGal). This indicates that the factors in Table 1 not applicable to internal COEs give rise to a large amount of the total variance. For example, DC offsets resulting from mis-ties to

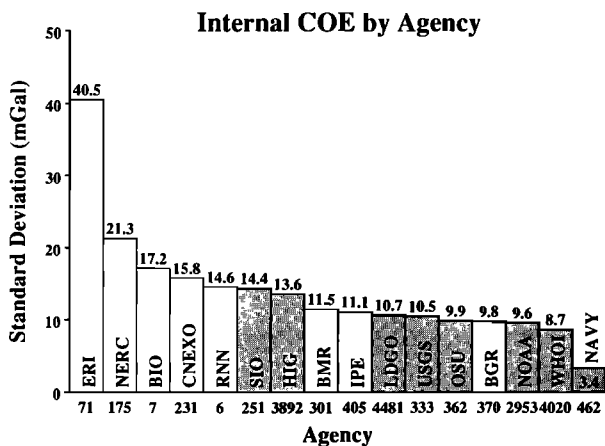


Fig. 6. Standard deviation of the internal COEs for each agency contributing to the data base. U.S. agencies are shaded. Note that the number of COEs used to calculate the standard deviation (listed below each column) varies substantially, so some of the variations are not very well constrained.

the base station will not give rise to an internal COE, but could contribute substantially to external COEs. We note that the 944 points outside the plot interval are responsible for much of this variance; if they were excluded, the standard deviation would drop to 12.36 mGal.

The 16 collecting agencies involved have different procedures for handling the reduction of raw gravity data to free-air anomalies, which could give rise to a different error level for each agency. To investigate such a possibility, we plotted the standard deviation based on internal COEs only for each agency, as shown in Figure 6. Most of them come out with a standard deviation of 10 ± 3 mGal. The ERI data give quite high COEs, which may reflect the high gravity gradients in the survey area (Japan trench). The U.S. Navy has the lowest COEs, with a standard deviation of 3.4 mGal. However, this value is probably biased, since a substantial part of the legs involved were grid surveys with many crossovers confined to a small area, which allows better constraints on the data reduction. There are also reasons to believe that the navigation system employed gives very accurate positioning.

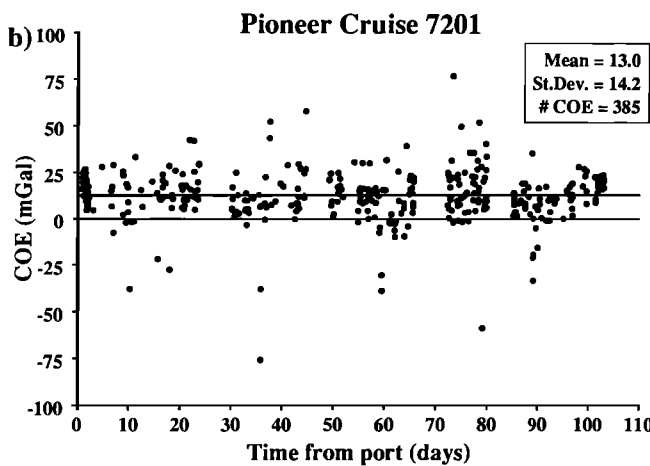
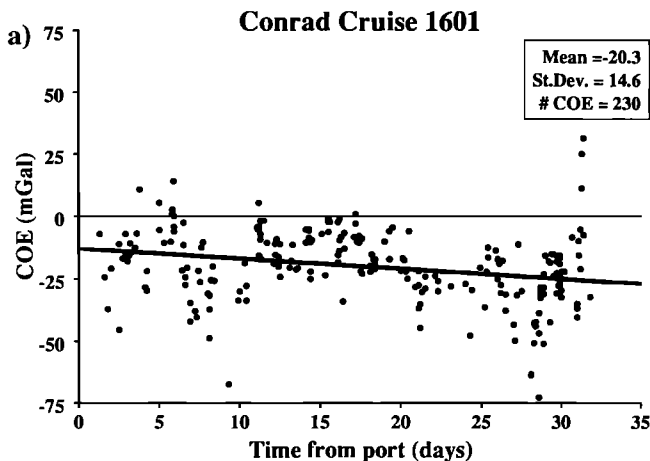


Fig. 7. (a) Plot of COEs as a function of time from port for *Conrad* cruise 1601 (1972) before correction. The heavy line is the regression line and indicates a drift rate of -0.4 mGal/d. Note that the regression line is everywhere below the zero line. (b) Plot of COEs as a function of time from port for *Pioneer* cruise 7201 (1972) before correction. There is no indication of tilt in the crossover data, but a 13 mGal bias is clearly seen.

THE DRIFT AND DC OFFSET PROBLEM

Since sea gravimeters only provide measurements of relative gravity, it is essential to connect the meter readings to a world wide network of gravity stations. If this tie-in prior to leaving the port is somehow incomplete or not performed at all, the resulting gravity field will be off by a constant factor along the entire leg. Moreover, most gravimeters tend to drift with time, thereby introducing systematic errors in the gravity measurements. The standard way to suppress this distortion is to tie in the gravimeter to the local network at the end of the cruise, and then check if the meter reading and base station values agree. If they do not agree, the offset is assumed to be due to linear drift, which is then removed from the raw measurements. Errors in any of the two tie-ins will therefore produce an artificial drift rate, leaving a tilt and/or a DC offset in the reduced free-air anomaly.

Another difficulty is that over the years, different reference gravity formulas have been used to reduce the raw observations to free-air gravity anomalies. For example, the 1930 International Reference Ellipsoid was used widely by

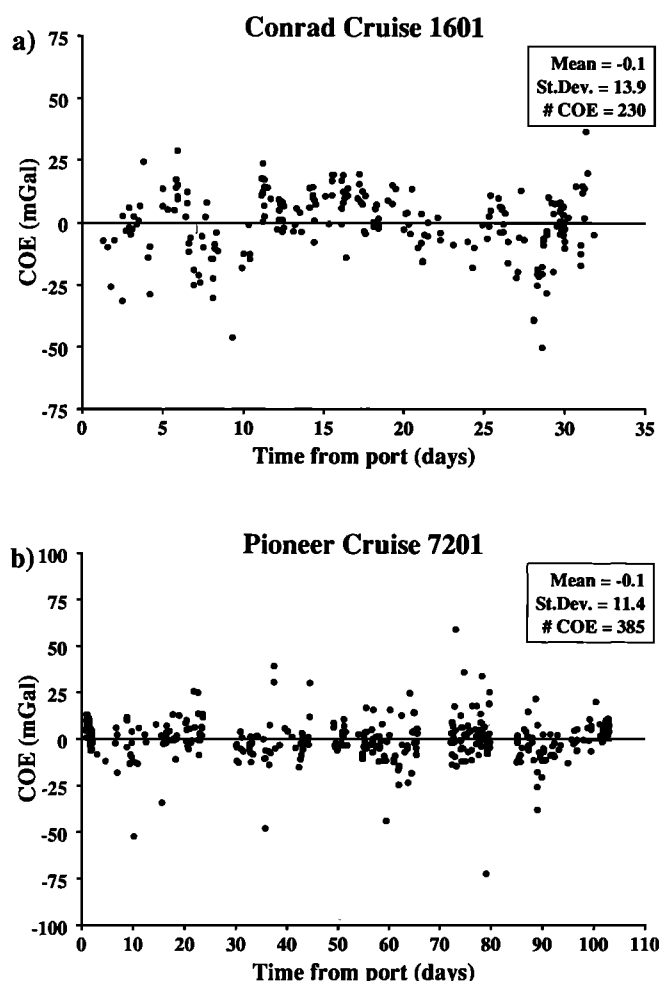


Fig. 8. (a) Plot of COEs as a function of time from port for C1601 after correction for tilts and DC shifts. The -0.4 mGal/d drift rate has been removed, and the mean of the COEs is close to zero. Note that the standard deviation also has dropped, from 14.6 mGal in Figure 7a to 13.1 mGal after adjustment. (b) Plot of COEs as a function of time from port for P7201 after correction for tilts and DC shifts. The 13 mGal bias has now completely been removed, and the standard deviation has been reduced from 14.2 to 10.6 mGal.

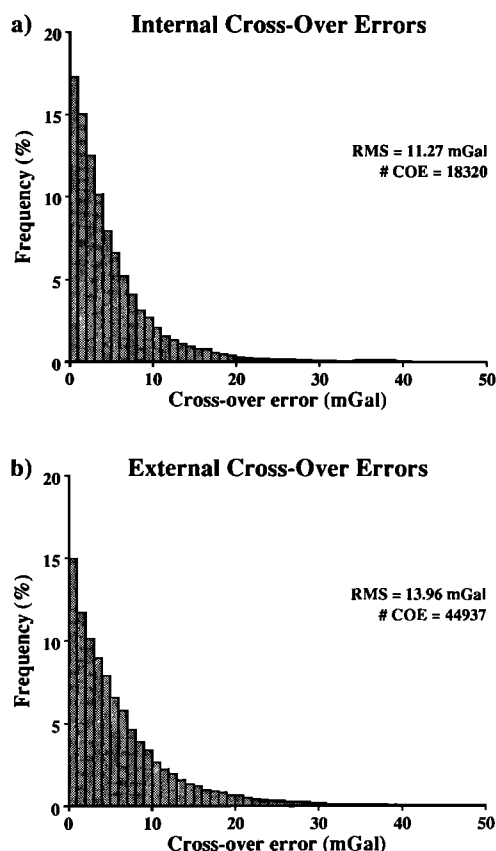


Fig. 9. (a) Histogram of internal COE for all legs after adjusting for tilts and DC shifts. The distribution looks similar to the one prior to adjustments, indicating that instrument drift has been properly dealt with by most agencies at the time of initial data reduction. (b) Histogram of external COEs for all legs after crossover correction. The new distribution is clearly narrower, indicating that a significant portion of the COEs was due to DC shifts.

collecting agencies for a few decades. The switch to more accurate formulas incorporating satellite-derived values for the Earth's ellipticity, however, was slow and occurred at different times for different agencies. Since this information is not always available, systematic differences in the form of DC shifts may be expected between legs.

We have found that both tilt and DC shift are present in our data set, here exemplified by two legs, R/V *Conrad* cruise C1601 and *Pioneer* cruise P7201. Figure 7 shows COEs generated between these legs and all other legs that intersect them, plotted as a function of days since leaving port. In the case of C1601, we observe that the magnitude of the COEs systematically increase with time. The regression line plotted indicates a drift rate of -0.41 mGal/d, accumulating to more than 13 mGal by the end of the cruise. Also, most COEs are negative (since mean COE = -20.3 mGal) suggesting that the entire cruise is offset relative to the other legs crossing it. The *Pioneer* leg shows no systematic change for the duration of the cruise, but the mean COE is off by 13 mGal.

Obviously, in order to compare several cruises in the same area (e.g., preparing free-air anomaly maps), it is necessary to correct for any systematic errors in the data. In order to make the data set more consistent, we applied a two-step iterative method. First, we computed the regression line (i.e.,

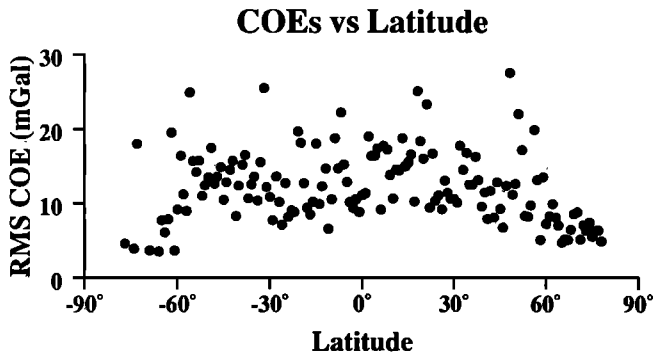


Fig. 10. The rms of the external COEs, computed over all longitudes, plotted against latitude. The COEs seem to be higher at low latitudes and decrease toward the poles, as predicted by (4).

as in Figure 7) for each leg, then removed these systematic trends from each of the legs, and finally recomputed new regression lines. This loop was performed until convergence was obtained, typically after 5–6 iterations. Fortunately, most legs have the bulk of their COEs near ports of departure and arrival, thus making a stable estimation of the slopes possible. However, legs with a small number of COEs tend to yield quite arbitrary drift rates. To prevent this, we used a cutoff number of 100 COEs. For legs with less than 100 COEs, no drift rate was computed. To check for unusual cases, the COE versus time from port were plotted for the remaining ~300 legs, and these plots were used to select the

legs for which a tilt correction seemed justified. Second, a similar iteration scheme was employed to find the DC offsets. Here, however, the legs were given different weights according to their performance (as measured by their standard deviation) in the internal crossover analysis, the weights also being proportional to the number of COEs involved for each leg. The whole two-step procedure as outlined above has the effect of reducing the overall standard deviation in a weighted least squares sense by removing the offsets and drift rates. After these corrections, no significant tilt was found in the data set. Figure 8 shows the effect of the corrections on the gravity data for legs C1601 and P7201 after the adjustments have been applied to all legs. We see from the figure that there is now no drift present in the C1601 data, and both legs have a mean COE close to zero. Also note that their standard deviations have decreased substantially.

The most dramatic change overall occurs for the external COEs in Figure 9. The distribution has clearly been narrowed, reflecting the 38% drop in standard deviation to 13.96 mGal. Now, only 528 COEs fall outside the plotting interval, and this improvement contributes the most to the reduced deviation. For the data inside the plotting window, the new standard deviation is 10.04 mGal, a 19% improvement over the corresponding value prior to correction. The internal COEs, on the other hand, have only been slightly affected. Except for a 0.02-mGal drop in standard deviation, the distribution looks similar to the one we found prior to corrections. This indicates that the DC correction played a

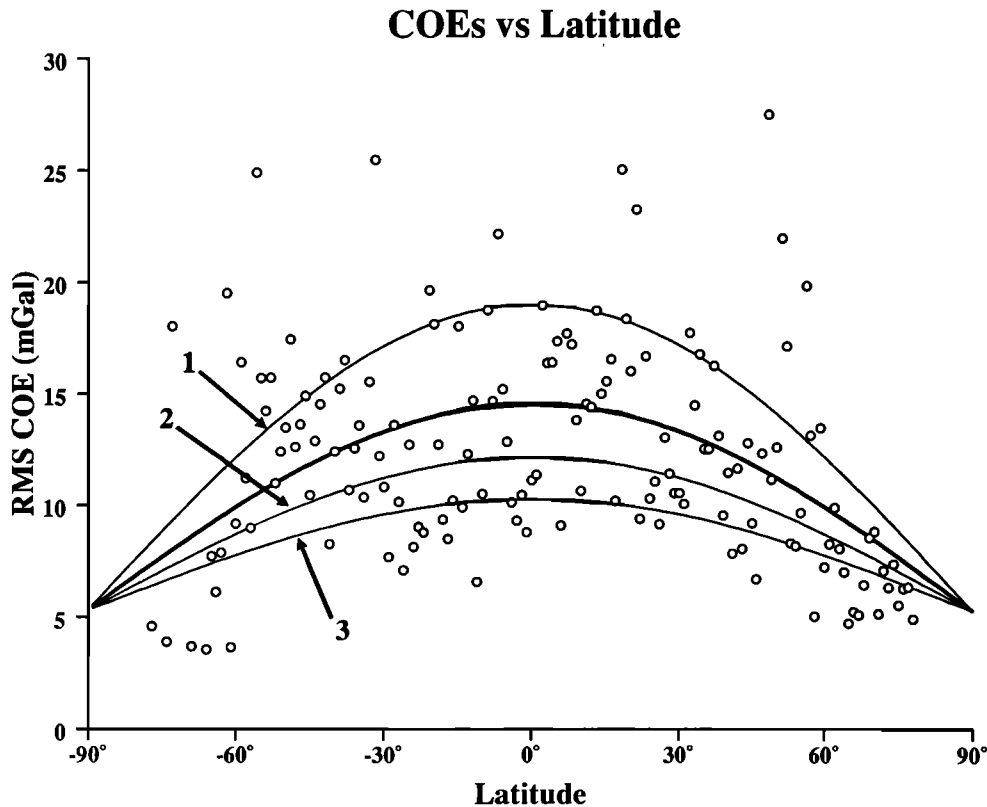


Fig. 11. Same data set as in Figure 10 with a family of curves representing different choices for $\Delta\alpha$ and Δv . The best fitting heavy line can be parameterized by $\Delta\alpha = 4^\circ$ and $\Delta v = 0.5 \text{ m s}^{-1}$. For the other curves, the values are (1) 6° and 0.75 m s^{-1} , (2) 3° and 0.4 m s^{-1} and (3) 2.5° and 0.25 m s^{-1} .

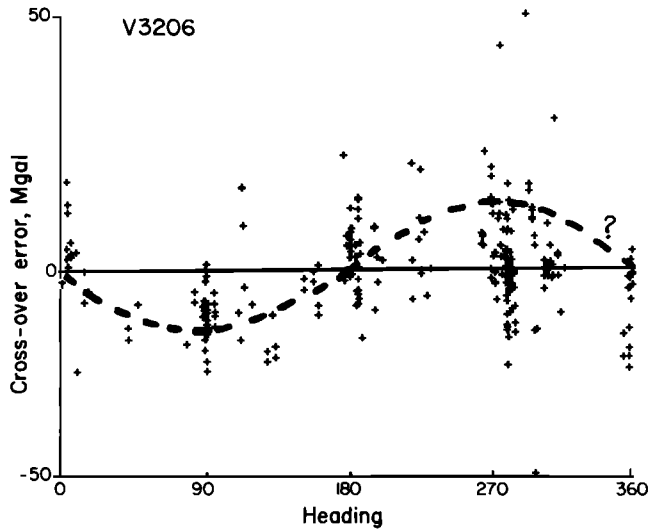


Fig. 12. Plot of external COEs versus the ship's heading for *Vema* cruise 3206 (1975). A sinusoidal pattern can be detected but could not be parameterized accurately enough to justify a correction.

far more significant role than the tilt correction, since only the latter would affect the internal COEs.

RESIDUAL CROSSOVER ERRORS

As Figure 9 shows, errors still remain in the data set even after the drift and DC corrections have been applied. These errors must be attributed to other factors such as those listed in Table 1. It is generally assumed that poor navigation is a major source of uncertainty for sea gravity measurements. In addition to determining the position of individual points, the navigation also enters directly in the data processing through the Eötvös correction. This correction restores the gravity measurements to what they would be if the ship had not been moving, and is of the form

$$E = 14.585v \cos \phi \sin \alpha + 0.015696v^2 \text{ (mGal)} \quad (1)$$

where v , α , and ϕ are the ship's speed (in m s^{-1}), heading and latitude, respectively [e. g., *Dehlinger*, 1978].

In order to investigate whether COEs vary with latitude, we computed the standard deviation of all external COEs within 1° latitude bands and plotted the result as a function of latitude. This is illustrated in Figure 10. The COEs clearly decrease from the equator toward the poles. To be able to explain this systematic dependence on latitude, we used a model of a typical COE as in Figure 4. One possible source of error would be uncertainties in the Eötvös correction. Differentiating (1) with respect to latitude, heading, and speed, we get

$$\Delta E = 14.585 \cos \phi (\Delta v \sin \alpha + v \Delta \alpha \cos \alpha) + 0.031392 v \Delta v \text{ (mGal)} \quad (2)$$

where $\Delta \alpha$ and Δv represent uncertainties in the ship's heading and speed, respectively, and terms containing $\Delta \phi$ have been ignored (they contribute less than 0.01 mGal). As a function of the ship's heading α , this expression has a mean value of $0.031392v\Delta v$, since the sine and cosine terms average to zero over a 360° interval. To find the standard deviation, we compute the variance of (2) over the 360° range and find

$$\sigma_{\Delta E} = 10.312 \cos \phi \sqrt{\Delta v^2 + v^2 \alpha^2} \text{ (mGal)} \quad (3)$$

Assuming that, on the average, the two ships involved in a crossover have the same velocity v and uncertainties Δv and $\Delta \alpha$, the standard deviation of that part of the COE due to incomplete Eötvös correction is therefore given by the standard error of the difference between two means, i.e.

$$\sigma_x = \sqrt{2} \sigma_{\Delta E} = 14.585 \cos \phi \sqrt{\Delta v^2 + v^2 \Delta \alpha^2} \text{ (mGal)} \quad (4)$$

Figure 11 shows the COEs as a function of latitude, and with three curves corresponding to reasonable combinations of Δv

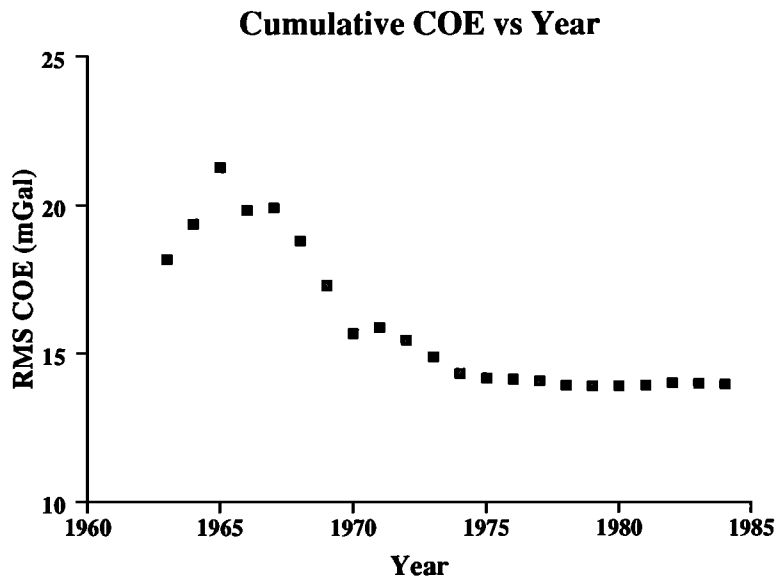


Fig. 13. Plot of the rms value of all COEs for each year. Only COEs present from 1960 and up to the year in question were used in the calculation, resulting in a cumulative curve for the improvement of the accuracy of marine gravity measurements with time.

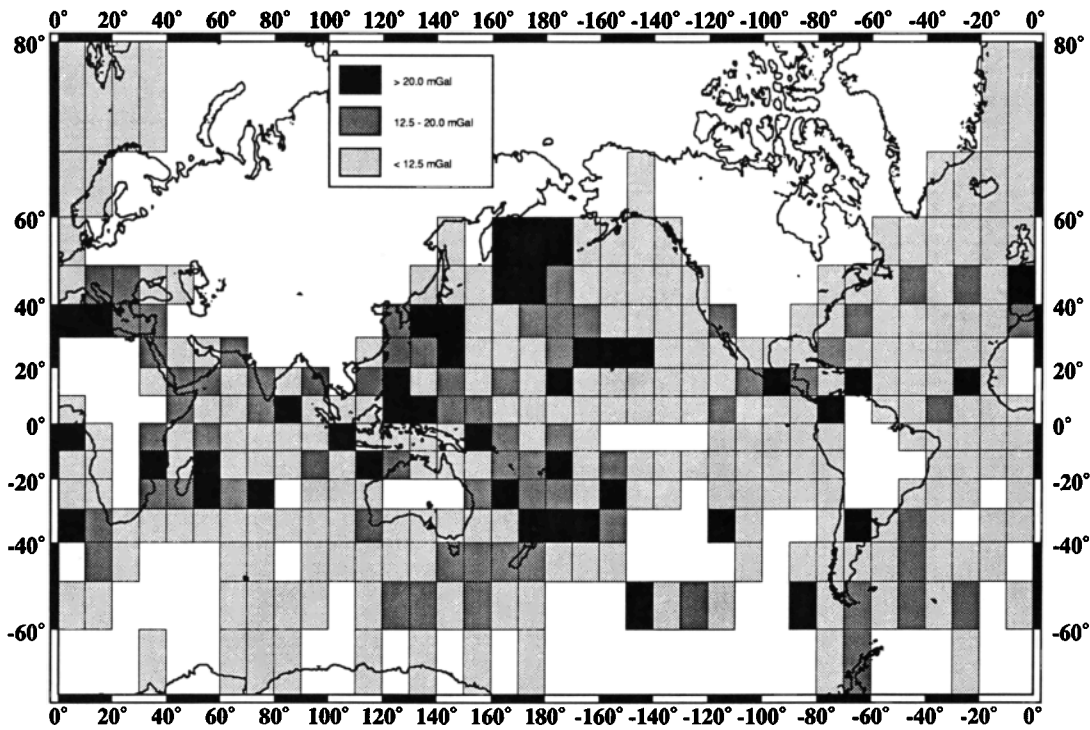


Fig. 14. Map showing the standard deviation of COEs within individual 10° by 10° blocks. High COE values seem to correlate with regions of rapidly varying high-amplitude gravity field, whereas low values are generally found over the abyssal plains. Intermediate COEs are found along continental margins. The white regions have no COEs.

Uncorrected - Corrected Data vs Grid Size

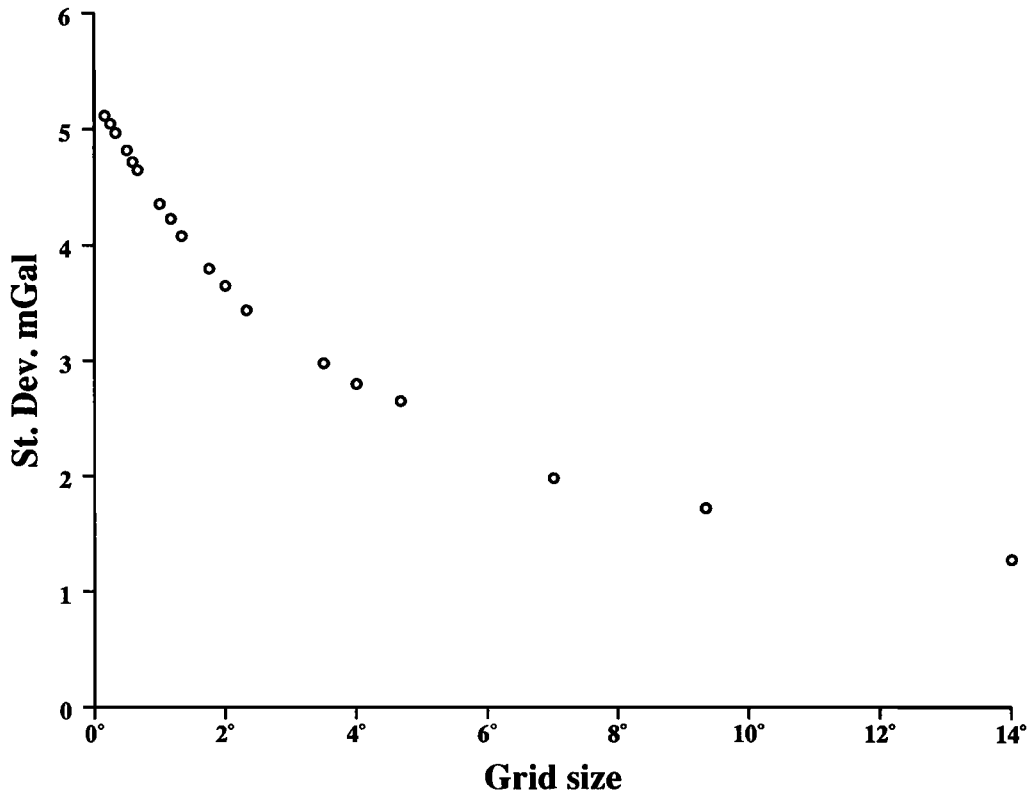


Fig. 15. Plot of the average standard deviation of the differences between the corrected and uncorrected data as a function of grid size for six different 28° by 28° areas. The differences are largest for small grid sizes, which suggests that the crossover adjustments improved the marine gravity measurements' ability to resolve short wavelength signals.

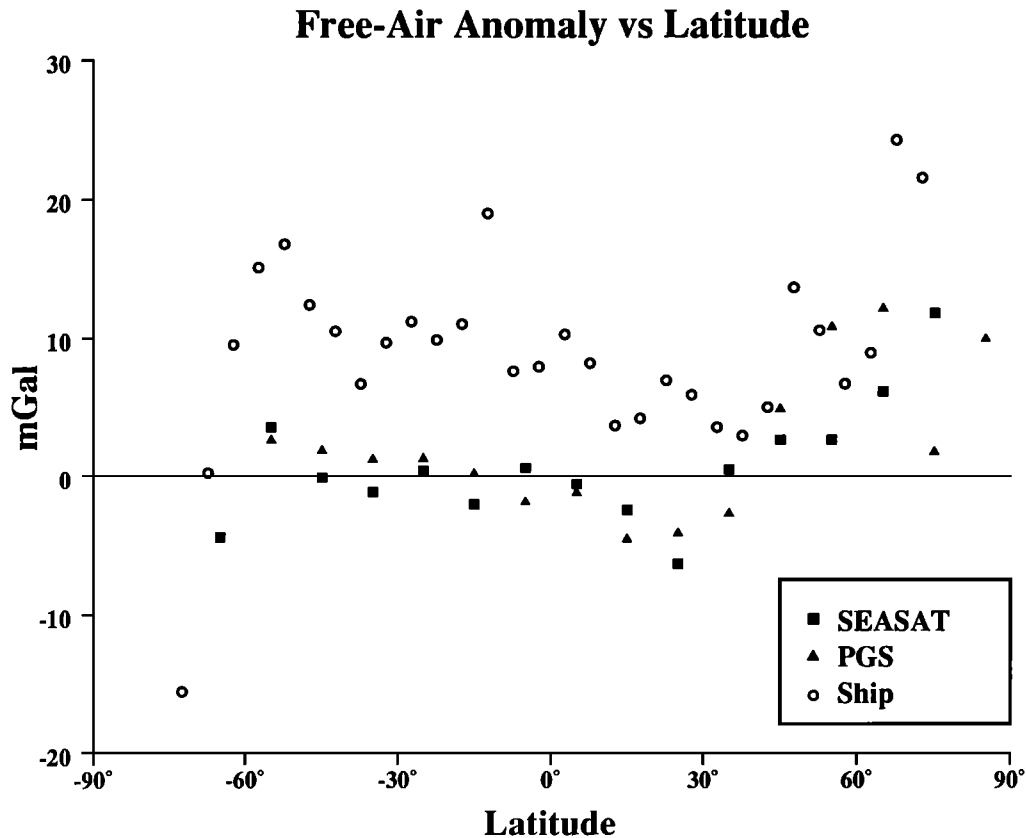


Fig. 16. Free-air anomalies, averaged over longitude, plotted against latitude. Only marine gravity data are plotted. Open circles denote marine gravity measurements, solid squares represent the Seasat-derived gravity field, whereas the black triangles are based on the PGS-1331 geopotential model. The difference between the marine data set and the satellite-derived fields is close to +9 mGal for all latitudes.

and $\Delta\alpha$ using (4) and assuming $v = 5 \text{ m s}^{-1}$. The solid line represents the best fitting cosine curve offset by the best fitting constant. This curve is consistent with an uncertainty of 4° in heading and 0.6 m s^{-1} in velocity, but any combination of Δv and $\Delta\alpha$ that give the same value for the square root will follow the same curve. Thus, Δv and $\Delta\alpha$ cannot be resolved from the data set. Even if we knew Δv and $\Delta\alpha$, we would not be able to go back and make any corrections in the original measurements because we still would need to know the direction of the uncertainties. Also, any estimate of these parameters would be of little value along the segments between crossover points.

We note that (4) predicts a zero COE due to incomplete Eötvös correction at the poles. This is obviously not the case in Figure 11. When the best fitting cosine curve had been removed from the data in Figure 11, we computed the autocorrelation function of the residual. We found that there was no significant latitudinal dependence left. Thus this background noise level of 5–6 mGal represents errors due to the remaining factors in Table 1.

One factor thought to be responsible for part of the COE is the cross-coupling effect. This error is common to all beam-type gravimeters (e.g., the LaCoste & Romberg and Graf-Askania meters) with which most of the marine gravity data have been collected. Cross-coupling occurs when the beam or the platform is not level. In that case, the horizontal accelerations of the ship will have a component perpendicular to the beam, and this will be indistinguishable from the vertical

accelerations. The magnitude of the cross-coupling error depends on the ship's heading into the sea, and *Talwani* [1966] showed that, on the average, its effect is proportional to

$$0.5X \phi \cos\theta \quad (5)$$

where X is the amplitude of the surge accelerations for some period, ϕ is the amplitude of the same periodic part of the beam motion (in radians), and θ is the phase angle between the surge and the beam. For a constant surge direction, the cross-coupling effect will vary periodically with the ship's heading. Thus we looked for legs where the COEs seemed to follow a sinusoidal curve when plotted against heading. Unfortunately, for all but a few legs, the distribution of COE with heading does not permit a sufficiently accurate parameterization of the curve. Figure 12 shows, however, a case for *Vema* cruise 3206, where a sinusoidal behavior can clearly be detected. Because of the uncertainty in determining the exact form of the cross-coupling error, we chose not to attempt corrections for this source of error. However, when working on a smaller area where ship track segments are straight lines, this correction could be included in the DC shift procedure, since its effect is more or less constant along lines of constant heading [*Prince and Forsyth, 1984*].

Improvements in instrumentation and quality of navigation would suggest that the accuracy of the sea gravity measurements should improve with time. Figure 13 shows the rms of all crossovers generated by cruises from 1960 and up to a

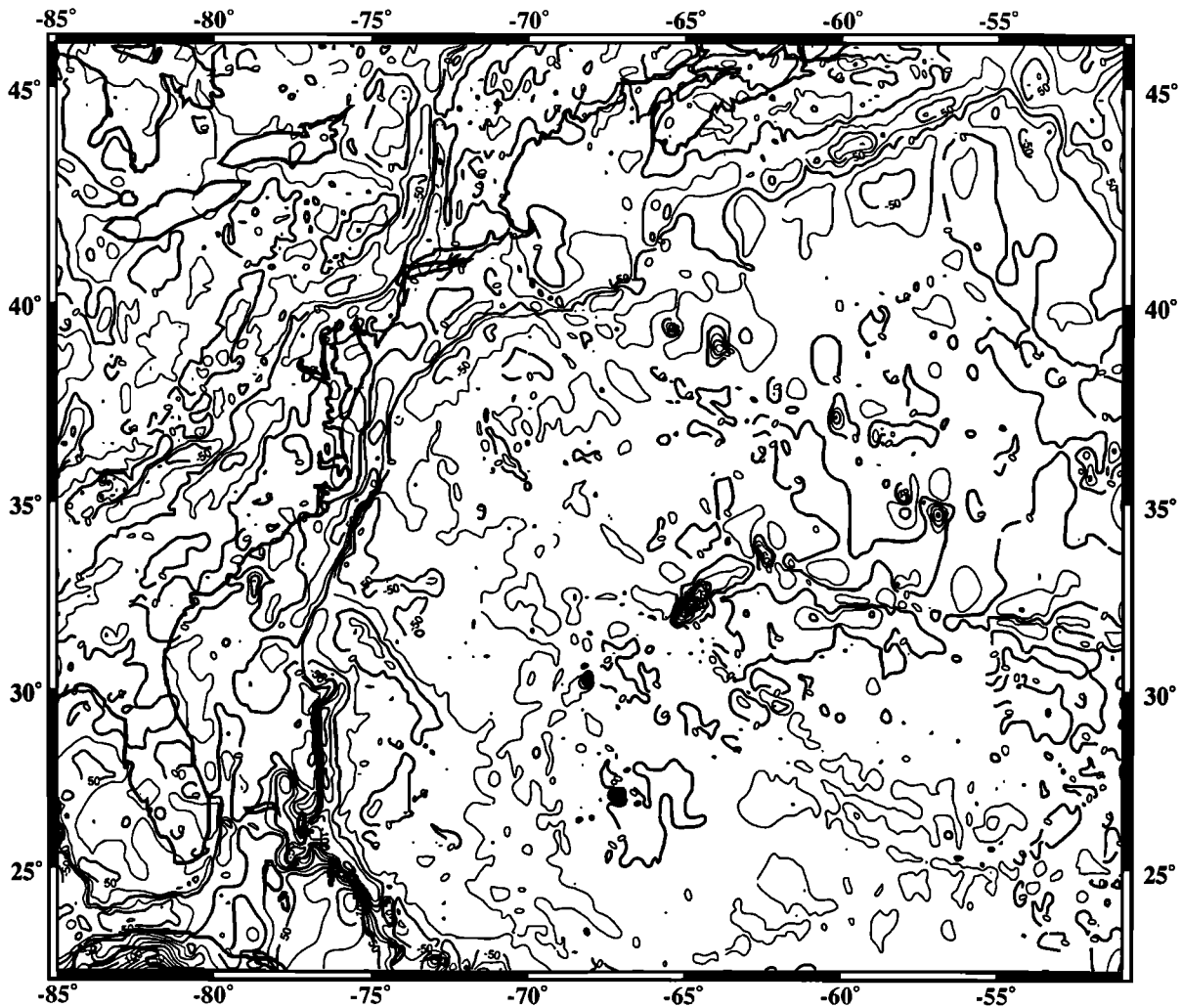


Fig. 17a. A 5' by 5' free-air anomaly map of the northwestern Atlantic Ocean and the eastern parts of the continental United States. Contour interval is 25 mGal. The map was compiled by the method described in the text. The heavy line outlines the land areas.

certain year plotted as a function of time. There is a clear trend in the data, indicating that the quality of gravity measurements has improved over time. The figure suggests that COEs dropped substantially during the years following the introduction of the TRANSIT satellite navigation system in 1967. A clear-cut "step" cannot be seen, however, probably because the transition to this new system actually took several years for some collecting agencies. Preliminary results from use of the new high-quality navigation NAVSTAR GPS [Ligon, 1985] and R/V *Conrad's* BGM-3 gravimeter [Bell and Watts, 1986] seem to indicate that sub-Gal accuracies are within reach, which would eventually reduce the total standard deviation of the data set.

Navigation affects the accuracy of the gravity measurements in two ways. One is through the Eötvös correction discussed above. The other is the fact that positions are determined by navigation. Due to poor navigation, the apparent crossover point may not be a single point, but two points separated by a small distance. In this case we are comparing gravity at two different locations, and this horizontal offset introduces an additional error which depends on the local gravity gradient. We may therefore expect the magnitude of COEs to

be correlated with areas of steep gravity gradients, particularly convergent plate boundaries and other areas of rapid variations in bathymetry, not fully compensated by isostatic mechanisms. This is confirmed in Figure 14, which shows the standard deviation of all external COEs within each 10° by 10° block. We note that there is a general tendency for high values to be associated with trenches, intermediate values with continental margins and seamounts, and low values with abyssal plains.

To see what effect the crossover corrections have on gridded data, we made several gridded data sets in different parts of the oceans. For each area, two gridded data sets were compiled based on the uncorrected and corrected gravity measurements, respectively. Then the differences between these two fields, for a given grid size, were computed for each area, and the standard deviation of the differences was calculated as a function of grid cell size. The results for the six areas were averaged and plotted in Figure 15. We see that the highest discrepancies occur at short wavelengths (0–750 km). This, together with the improvement in overall COE, suggests that the short wavelength features of the gravity field are better resolved by the corrected data set.

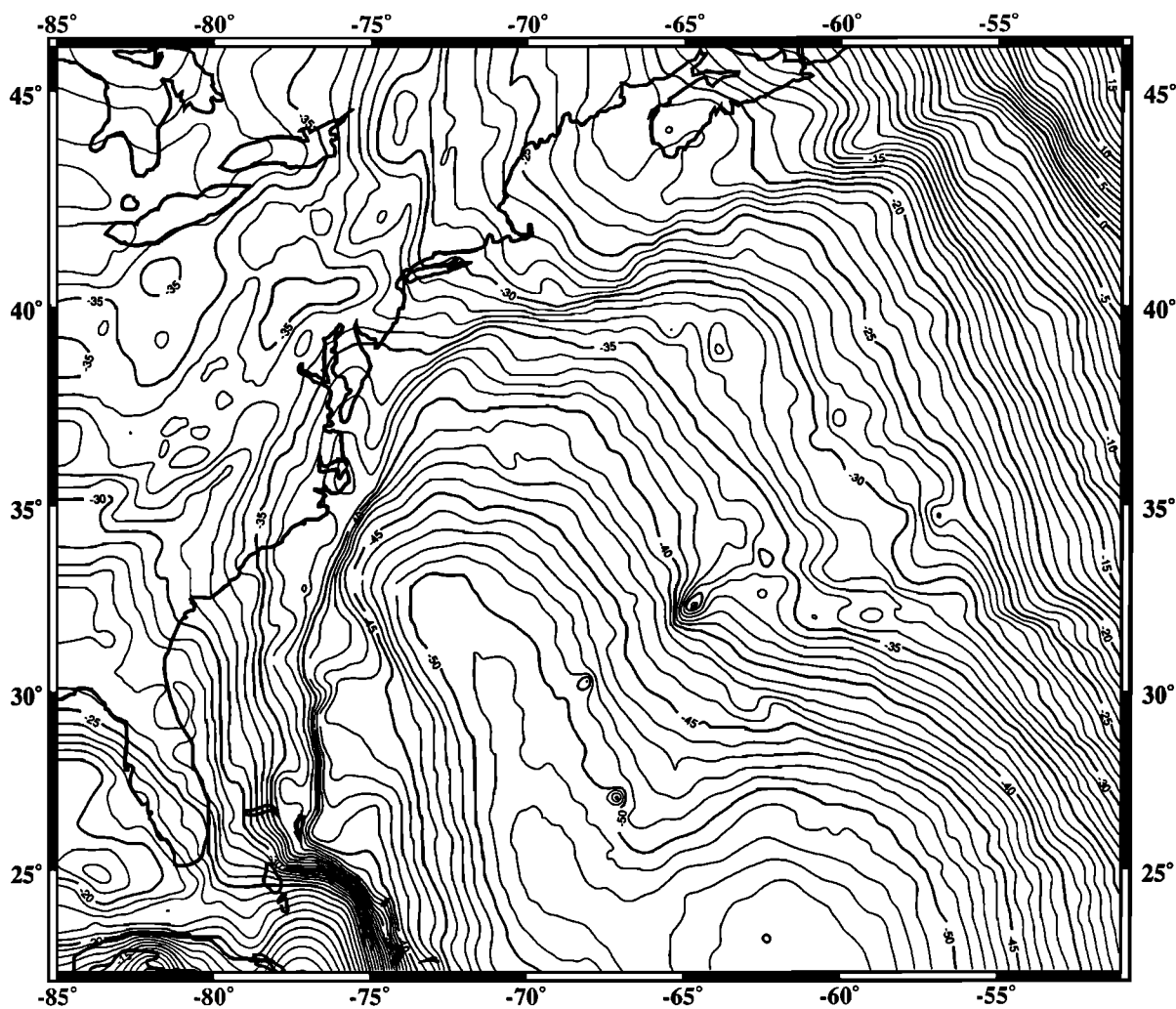


Fig. 17b. A gravimetric geoid for the same area, based on the free-air anomalies in Figure 17a. Contour interval is 1m. Long wavelength trends are added from the PGS-1331 geopotential model.

In order to evaluate the resolution of the corrected data set at long wavelengths (> 750 km), we compared the corrected and uncorrected data sets to gravity data derived from Seasat altimeter measurements (W. F. Haxby, manuscript in preparation, 1987). This comparison revealed that the corrected data set gave a smaller standard deviation than the uncorrected set, the difference amounting to 0.7–1.3 mGal for all wavelengths. We conclude therefore that the corrected data better resolve not only short wavelengths, but also the long wavelength gravity field.

A somewhat surprising result from comparison of the terrestrial and satellite-derived gravity fields was the presence of a bias in the marine data sets. The bias was found in both the uncorrected and corrected data sets and could not have been introduced by the COE corrections. To examine the full extent of this phenomena, we have investigated how the free-air anomaly varies with latitude, i.e., for each band of latitude, we computed the average value using data over the oceans only, and plotted them against latitude. This was done for both the marine data set and the Seasat-derived gravity. As an independent check, we also computed the low-order gravity field (complete to order and degree 24) from the PGS-1331 potential model [Marsh *et al.*, 1985], and the

results are displayed in Figure 16. The striking feature here is the nearly constant offset of +9 mGal in the terrestrial data set. We do not know the cause of this bias but speculate that it is partly due to uncertainties in choice of reference field (i.e., some legs have a Potsdam correction, while others have not), and partly due to a sampling bias, since most cruises tend to survey geologically interesting areas, which usually are associated with anomalous gravity values.

ERROR BUDGET

Having isolated some of the effects that contribute to the total COE standard deviation, we can set up a crude error budget indicating the relative importance of these error sources. The following budget is based on an initial standard deviation of 12.4 mGal, where the high COEs outside the $<-50,50>$ mGal interval have been ignored. This standard deviation represents 98% of the COEs found in this investigation. For a typical block at mid-latitudes we therefore find that COEs are ~20% due to drift/DC shift problems, ~40% due to incomplete Eötvös correction, and ~40% due to other sources (positioning, cross-coupling, etc.). Of these errors, the drift/DC shift effects were the only ones we were able to reliably remove. Thus for a typical area, the standard

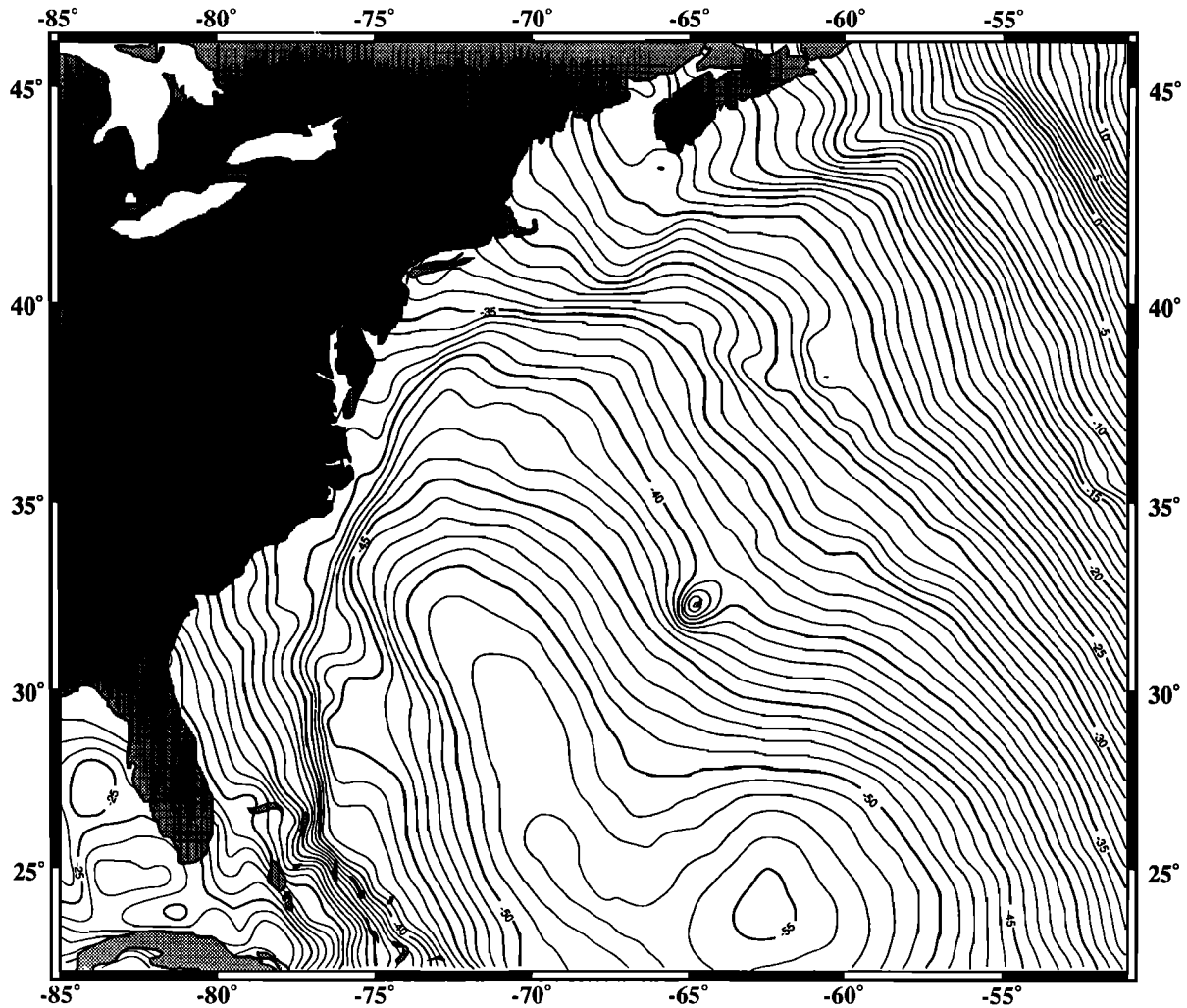


Fig. 18. Instantaneous sea surface heights derived from Seasat altimetry. Contour interval is 1 m. Values over land regions have been masked.

deviation would be ~ 10 mGal. However, when investigating a smaller area, more detailed adjustments can be made and a better value of the standard deviation might be calculated, thereby allowing a smaller contour interval to be applied [e.g., Prince and Forsyth, 1984].

DISCUSSION

The COE analysis technique developed in this paper has now enabled us to revise our algorithms used to grid marine gravity data. Instead of taking the arithmetic average of all the values within a certain block, the COE analysis allows us to give the individual legs different weights in addition to correcting for the drift/DC shift effect demonstrated above. To generate a regular grid of block average anomalies, we compute the weighted mean of the positions and the adjusted gravity measurements within each block. This scheme honors point values from cruises with low standard deviation of COEs, and likewise suppresses cruises with high COEs. Finally, we interpolate the anomalies at the desired grid intersections using a minimum curvature method [Briggs, 1974; Swain, 1976].

The adjustments applied to the gravity measurements from individual ship legs are by no means final, of course, and we

plan to update them as more measurements are added to the data bank. In practice, instead of correcting each individual measurement, we store the tilt and DC shift information in a master file and apply the appropriate corrections only when data are read from the data base. A complete list of the tilt and DC shift information required for all 834 legs examined in this paper can be found in the appendix.

Marine gravity measurements have been extensively used by geophysicists, geodesists, and geologists to investigate a wide range of phenomena, including lithospheric processes, potential field modeling, and oceanography. As an example, we constructed a new detailed gravimetric geoid for the northwestern Atlantic Ocean. All the available gravity data for this region have been corrected for COEs, averaged, and interpolated onto a 5' by 5' grid according to the scheme outlined above. The resulting free-air gravity anomaly map is shown in Figure 17a. In order to compute the gravimetric geoid, we first subtracted the long wavelength field, complete to order and degree 24, based on the PGS-1331 geopotential model. The difference gravity was then used to compute a difference geoid by first resampling the data to allow for the change in grid-cell area with latitude, and then applying a fast Fourier transform (FFT). Prior to taking the

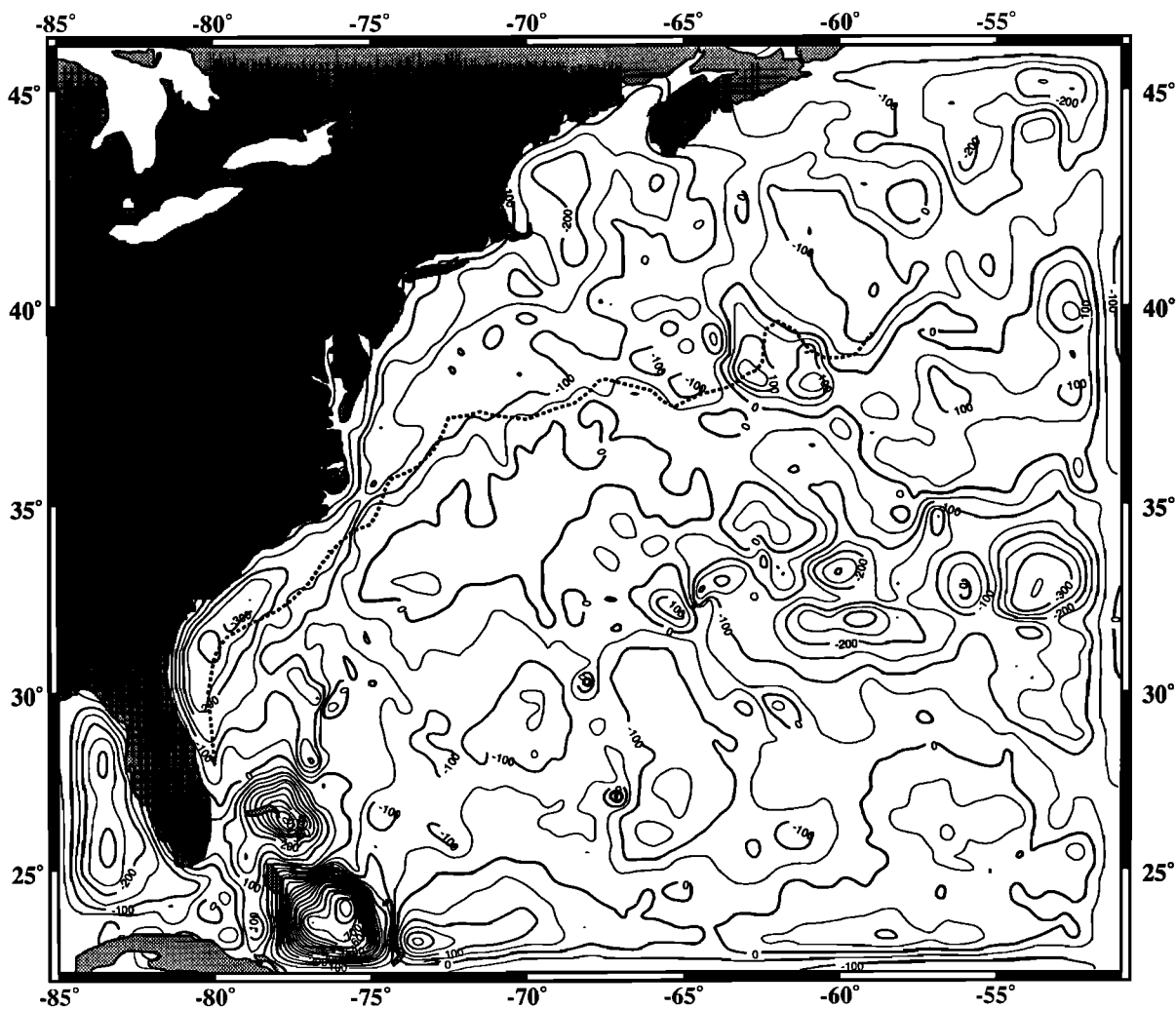


Fig. 19a. Residual geoid computed by subtracting the gravimetric geoid from the Seasat sea surface heights and high-pass filtering the difference. Contour interval used is 50 cm. Details along the edges are obscured due to tapering of the data prior to filtering in the wave number domain. Note the many correlations with seafloor topography in Figure 19b. The heavy dashed line indicates the approximate position of the frontal boundary of the Gulf Stream.

FFT, the best fitting plane was removed from the difference gravity, and the slopes around the edges tapered. Once in the wave number domain, it is straightforward to compute the geoid using Brun's formula by multiplying by $(\gamma k)^{-1}$, where γ is normal gravity and k is wave number. The gravimetric geoid was finally obtained by transforming back to the space domain and resampling the values at the original positions. While this method, being an improved flat Earth approximation, is less accurate than a full spherical harmonic treatment, it is computationally much faster. For the area in question, the error induced by using this technique is $\sim 5\%$ for the longest wavelengths, and the errors in the shorter wavelengths are negligible (W. F. Haxby, personal communication, 1987). The resulting difference geoid was then added to the long wavelength geoid based on the PGS-1331 model to obtain a total gravimetric geoid (Figure 17b).

Previous studies [e.g., Wunsch and Gaposchkin, 1980; Cheney and Marsh, 1981; Zlotnicki, 1984] have pointed out the potential use of gravimetric geoids in separating the temporal component in the instantaneous sea surface height derived from altimeter data. However, most of these studies

concentrated on the analysis of individual satellite tracks. Figure 18 shows the instantaneous sea surface for the region based on Seasat altimeter data. In order to investigate whether the improved gravimetric geoid could better separate temporal components in the altimeter data, we subtracted the gravimetric geoid from the altimetric geoid and high-pass filtered the difference to obtain a residual geoid (Figure 19a). Ideally, such a residual geoid should reveal those contributions to the Seasat-derived altimetric geoid that are not caused by the Earth's gravity field. Figure 19a reveals, however, several features of the residual geoid which correlate closely with topographic features on the seafloor (Figure 19b). For example, the smooth trend of the New England Seamount chain can be discerned in the residual geoid. We attribute such a correlation to the fact that the ships and the satellite did not sample their data at exactly the same locations, i.e., the gravimetric signature of some seamounts was picked up by the shipboard meters and missed by the satellite, and vice versa. Another problem is the inability of altimeter data to adequately resolve the short wavelength ($< 30\text{--}50$ km) features of the gravity field

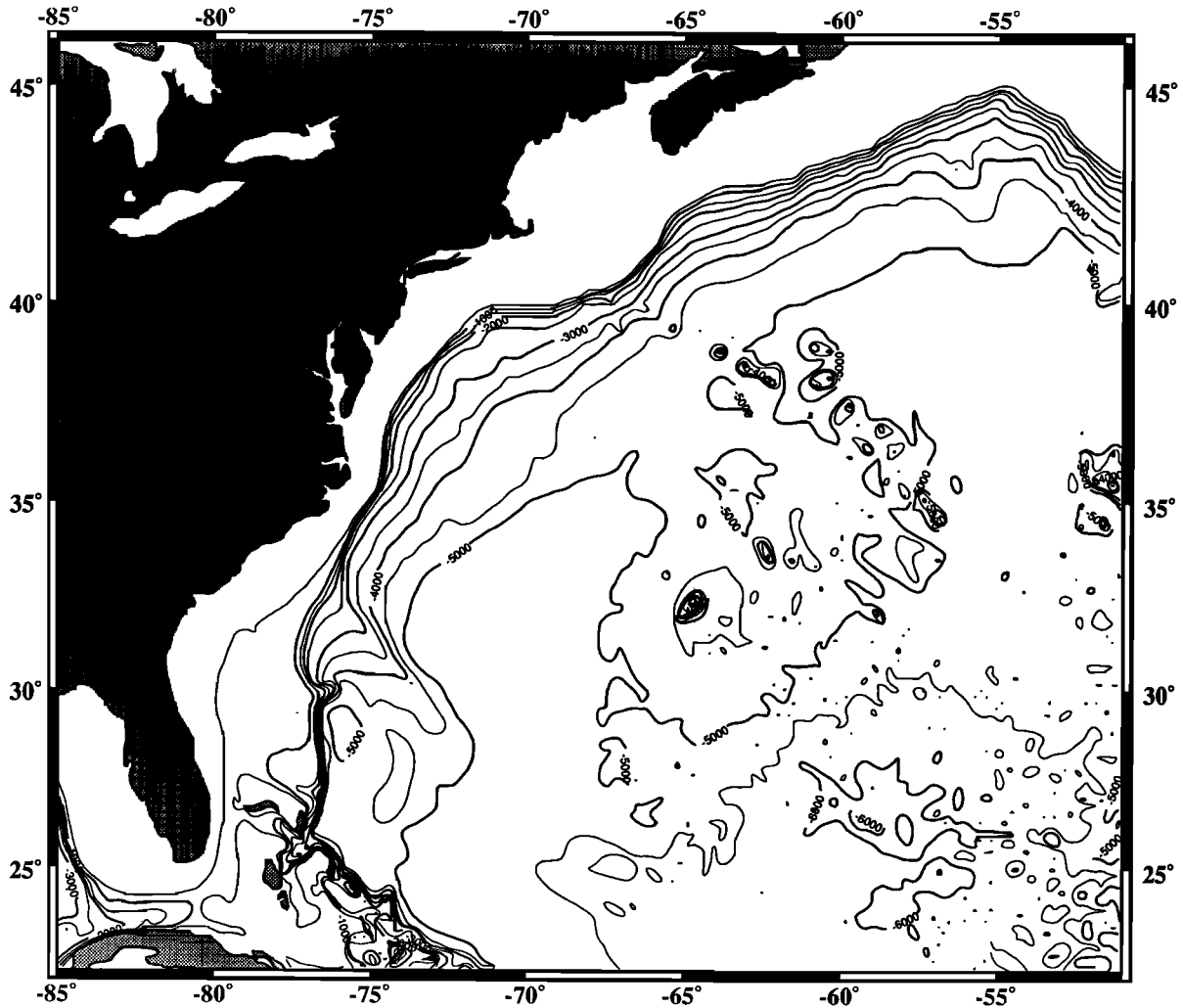


Fig. 19b. Seafloor topography, contoured at 500-m intervals, based on the DBDB5 5' by 5' gridded global topography data set.

[Brammer and Sailor, 1980]. Some features in the residual geoid, however, may correlate with temporal variables. The heavy dashed line in Figure 19a is the frontal boundary of the Gulf Stream as inferred from satellite infrared observations during the first 2 weeks of August 1978 [Cheney and Marsh, 1981]. The map shows a good correlation between the boundary and a gentle slope in the residual geoid which trends ENE from the shelf break off Cape Hatteras across the western Atlantic abyssal plain to the New England Seamount chain, where it becomes obscured.

SUMMARY

We have shown that the COE analysis approach enables us to monitor the quality of gravity data by "flagging" bad legs and optimizing the consistency of the global data set. Even though the accuracy of gravity measurements obtained is improving, the present rate of acquisition is such that only a relatively small number of measurements are added to the data base each year. It is therefore of considerable importance to utilize the extensive data base that has been obtained in the past in current gravity field models and other applications. It is unlikely that there will be any significant improvement in ship board gravity data coverage of the world's ocean basins during the next decade. The advent of satellite altimetry has provided us with a relatively dense

coverage of sea surface heights from which the gravity field can be obtained, assuming the sea surface to be representative of the geoid. Due to the presence of oceanographic signals, this altimetric gravity field departs from the field recorded aboard surface ships. In addition, due to incomplete sampling and instrument noise, the shorter wavelengths of the gravity field are not very well represented in the Seasat data set. These circumstances argue for more surface gravity measurements, which represent the short wavelength field very well.

APPENDIX

To correct the gravity measurements for the DC shift and linear drift mentioned above, we use the values presented in Table A1. The leg identification number gives the unique name for each leg, start date means the zero time from which the drift is measured, DC shift (in mGal) is the constant that must be added to the data, drift rate is measured in mGal/d, and finally, weight is a factor from 1 to 10 reflecting the overall quality of gravity measurements belonging to this leg (the higher weight the better quality). The correction we must apply is then

$$G_{\text{corr}} = G_{\text{uncorr}} + (T_{\text{point}} - T_{\text{startdate}}) * \text{Driftrate} + \text{DCshift} \quad (\text{A1})$$

where $T_{\text{startdate}}$ refers to 0 hours, 0 min on the day indicated in Table A1.

TABLE A1. Crossover Corrections

Leg	Start Date	DC Shift	Drift Rate	Weight
22809	June 12, 1963	17.50	0.0000	5
22943	Oct. 2, 1963	4.80	0.0000	5
22945	Nov. 26, 1963	0.10	0.0000	5
22946	Jan. 2, 1964	2.30	0.0000	5
22947	Feb. 8, 1964	-12.40	0.0000	5
22948	March 1, 1964	0.90	0.0000	5
22982	May 8, 1964	4.10	0.0000	5
22983	Jan. 21, 1964	0.90	0.0000	5
22984	March 30, 1964	0.00	0.0000	5
22985	April 23, 1964	0.90	0.0000	5
A2490	Jan. 8, 1968	19.60	0.0000	1
A2671	Jan. 21, 1972	-2.50	0.0000	5
A2672	Feb. 4, 1972	-1.30	0.0000	5
A2673	Feb. 27, 1972	3.51	-0.2016	5
A2675	April 12, 1972	2.40	0.0000	5
A2676	May 10, 1972	-0.90	0.0000	5
A2677	June 4, 1972	-1.50	0.0000	5
A2731	Nov. 12, 1972	5.00	0.0000	5
A2753	March 12, 1973	-0.50	0.0000	5
A2754	April 8, 1973	0.20	0.0000	5
A2755	May 5, 1973	-1.10	0.0000	5
A2756	May 28, 1973	-8.54	0.3600	5
A2757	June 23, 1973	-2.40	0.0000	5
A2891	April 14, 1975	-1.50	0.0000	5
A2892	April 30, 1975	-0.70	0.0000	8
A2893	May 18, 1975	-0.50	0.0000	8
A2931	Oct. 29, 1975	-3.30	0.0000	5
A2937	April 8, 1976	-0.20	0.0000	4
A9312	Sept. 2, 1976	0.00	0.0000	5
A9313	Oct. 1, 1976	0.00	0.0000	5
A9314	Oct. 29, 1976	-377.90	0.0000	5
A9317	Feb. 7, 1977	0.30	0.0000	2
A9318	March 3, 1977	0.76	0.0432	6
A9319	March 29, 1977	-4.40	0.0000	1
AKK05	Feb. 4, 1969	8.36	-0.0576	1
AKK15	June 20, 1973	-1.60	0.0000	3
AKK20	Feb. 12, 1975	-0.82	0.0288	6
AKK23	Sept. 28, 1976	0.60	0.0000	5
BAJ6A	July 3, 1976	0.40	0.0000	5
BAJ6B	July 14, 1976	2.68	-0.2016	5
BAJA5	July 6, 1975	0.14	-0.0144	3
BBAY2	April 16, 1970	0.00	0.0000	5
BMR05	Jan. 1, 1970	-0.93	-0.0144	1
BMR10	Jan. 1, 1971	-0.60	0.0000	5
BMR12	Jan. 2, 1974	4.55	-0.1008	2
BMR13	Jan. 1, 1972	-3.37	0.0144	2
BMR14	Jan. 11, 1973	-0.27	0.0720	2
BMR5A	Aug. 27, 1977	0.06	-0.0288	2
BOMDI	May 5, 1969	2.30	0.0000	5
BOW03	Sept. 17, 1969	0.30	0.0000	5
C0801	Nov. 26, 1963	8.20	0.0000	5
C0802	Jan. 5, 1964	7.00	0.0000	5
C0803	Feb. 6, 1964	6.10	0.0000	5
C0804	March 4, 1964	6.50	0.0000	5
C0806	March 16, 1964	13.20	0.0000	5
C0807	April 21, 1964	7.80	0.0000	5
C0809	June 1, 1964	1.00	0.0000	1
C0812	Aug. 5, 1964	9.50	-0.2736	5
C0901	Oct. 17, 1964	7.27	-0.1152	5
C0902	Nov. 12, 1964	4.20	0.0000	2
C0903	Dec. 10, 1964	-3.18	0.2592	2
C0904	Jan. 21, 1965	3.90	0.0000	5
C0905	Feb. 12, 1965	4.20	0.0000	5
C0906	March 23, 1965	20.90	0.0000	5
C0907	April 23, 1965	21.80	0.0000	5
C0908	May 15, 1965	0.00	0.0000	5
C0909	May 20, 1965	0.00	0.0000	5
C0912	July 29, 1965	5.10	0.0000	5
C0913	Aug. 27, 1965	3.60	0.0000	5
C1001	Dec. 1, 1965	-1.43	0.0144	5
C1003	Dec. 28, 1965	-0.76	0.2592	5
C1004	Jan. 28, 1966	5.10	0.0000	5
C1005	Feb. 25, 1966	0.10	0.0000	5

TABLE A1 (continued)

Leg	Start Date	DC Shift	Drift Rate	Weight
C1006	March 27, 1966	2.90	0.0000	5
C1007	April 28, 1966	-0.99	0.0432	5
C1008	June 9, 1966	3.80	0.0000	5
C1009	July 2, 1966	0.30	0.0000	5
C1010	July 16, 1966	3.30	0.0000	5
C1011	Aug. 14, 1966	3.00	0.0000	5
C1012	Sept. 13, 1966	-1.00	0.1296	5
C1104	March 2, 1967	21.80	0.0000	5
C1105	April 6, 1967	4.40	0.0000	5
C1106	May 12, 1967	-0.20	0.0000	5
C1107	May 20, 1967	2.60	0.0000	5
C1108	June 27, 1967	8.90	0.0000	5
C1109	July 14, 1967	4.30	0.0000	5
C1110	Aug. 20, 1967	0.30	0.0000	5
C1111	Sept. 19, 1967	1.80	0.0000	5
C1112	Oct. 21, 1967	1.97	-0.5184	5
C1201	Jan. 3, 1968	1.06	0.0576	5
C1202	Feb. 9, 1968	1.40	0.0000	5
C1203	Feb. 23, 1968	0.40	0.0000	5
C1204	March 28, 1968	-0.90	0.0000	5
C1205	May 1, 1968	1.10	0.0000	5
C1206	June 3, 1968	-1.70	0.0000	5
C1207	July 4, 1968	2.50	0.0000	5
C1208	July 21, 1968	1.20	0.0000	5
C1209	Aug. 14, 1968	5.20	0.0000	5
C1210	Sept. 10, 1968	-0.90	0.0000	5
C1211	Oct. 1, 1968	0.20	0.0000	5
C1212	Nov. 7, 1968	-0.60	0.0000	5
C1213	Dec. 20, 1968	2.70	0.0000	5
C1214	Feb. 2, 1969	2.50	0.0000	5
C1215	March 31, 1969	-3.60	0.0000	5
C1216	May 8, 1969	-8.00	0.0000	5
C1217	May 28, 1969	-3.20	0.0000	5
C1218	June 23, 1969	1.50	0.0000	5
C1219	July 12, 1969	0.30	0.0000	5
C1220	Aug. 9, 1969	-1.90	0.0000	5
C1301	Sept. 9, 1969	-0.60	0.0000	5
C1307	April 19, 1970	2.19	-0.0288	5
C1308	May 22, 1970	3.00	0.0000	5
C1309	June 20, 1970	0.00	0.0000	5
C1310	June 26, 1970	0.20	0.0000	5
C1311	July 31, 1970	9.59	0.2448	5
C1312	Sept. 2, 1970	9.00	0.0000	5
C1313	Oct. 3, 1970	7.72	-0.0576	5
C1314	Dec. 9, 1970	-3.70	0.0000	5
C1401	Jan. 17, 1971	-1.10	0.0000	5
C1402	March 3, 1971	-4.40	0.0000	4
C1403	April 6, 1971	-0.60	0.0000	5
C1404	May 9, 1971	0.90	0.0000	5
C1405	June 17, 1971	-1.10	0.0000	5
C1406	July 18, 1971	1.30	0.0000	5
C1407	Aug. 20, 1971	0.70	0.0000	5
C1501	Sept. 29, 1971	-0.90	0.0000	5
C1502	Nov. 1, 1971	-2.20	0.0000	5
C1503	Dec. 5, 1971	-0.20	0.0000	5
C1504	Jan. 5, 1972	-0.80	0.0000	5
C1505	Feb. 12, 1972	-0.90	0.0000	5
C1506	March 14, 1972	-1.00	0.0000	5
C1507	April 16, 1972	-2.50	0.0000	5
C1508	May 11, 1972	-3.58	0.1296	5
C1509	June 8, 1972	-2.30	-0.0288	5
C1510	July 6, 1972	-1.50	0.0000	2
C1601	Aug. 10, 1972	13.46	0.3744	1
C1602	Sept. 14, 1972	-0.40	0.0000	4
C1603	Oct. 14, 1972	-2.59	0.0576	5
C1604	Nov. 18, 1972	1.30	0.0000	5
C1605	Dec. 21, 1972	-2.40	0.0000	5
C1606	Jan. 24, 1973	-9.00	0.0000	5
C1607	Feb. 24, 1973	-4.56	0.1152	4
C1608	March 9, 1973	-2.30	0.0000	5
C1609	March 23, 1973	-3.10	0.0000	5
C1610	May 4, 1973	-0.20	0.0000	5
C1611	June 3, 1973	-4.52	0.2448	5

TABLE A1 (continued)

Leg	Start Date	DC Shift	Drift Rate	Weight
C1612	July 6, 1973	-0.59	-0.0864	5
C1613	Aug. 9, 1973	-1.18	0.0720	7
C1701	Oct. 9, 1973	0.30	0.0000	5
C1702	Nov. 1, 1973	-0.90	0.0000	5
C1703	Dec. 3, 1973	-4.30	0.0000	5
C1704	Jan. 5, 1974	-0.80	0.0000	5
C1705	Feb. 25, 1974	-3.50	0.0000	5
C1706	April 17, 1974	-3.60	0.0000	5
C1707	May 17, 1974	-2.30	0.0000	5
C1708	June 22, 1974	-6.07	-0.0864	5
C1709	July 27, 1974	-5.10	0.0000	5
C1710	Aug. 15, 1974	-6.41	0.1152	5
C1711	Sept. 16, 1974	0.28	-0.1728	5
C1712	Oct. 20, 1974	-1.70	0.0000	5
C1713	Nov. 22, 1974	1.10	0.0000	5
C1714	Dec. 22, 1974	0.90	0.0000	5
C1801	Feb. 2, 1975	0.70	0.0000	5
C1802	March 15, 1975	2.70	0.0000	5
C1803	April 15, 1975	2.30	0.0000	5
C1804	May 16, 1975	2.90	-0.2016	5
C1805	June 17, 1975	-3.30	0.0000	5
C1806	June 22, 1975	0.68	-0.0720	5
C1902	Aug. 13, 1975	0.00	0.0000	5
C1903	Oct. 22, 1975	2.00	0.0000	5
C1904	Nov. 23, 1975	-2.91	0.1152	5
C1906	Jan. 25, 1976	0.36	0.0288	5
C1907	Feb. 27, 1976	-1.20	0.0000	5
C2002	June 10, 1976	13.16	-0.2304	7
C2003	July 29, 1976	-3.80	0.0000	5
C2004	Aug. 25, 1976	2.50	0.0000	5
C2006	Oct. 26, 1976	5.30	-0.2880	5
C2007	Dec. 3, 1976	-5.50	0.0000	5
C2008	Dec. 23, 1976	-3.80	0.0000	5
C2009	Jan. 5, 1977	-3.30	0.0000	5
C2101	Sept. 9, 1977	0.70	0.0000	5
C2102	Oct. 2, 1977	1.50	0.0000	5
C2103	Nov. 10, 1977	8.30	0.0000	5
C2104	Dec. 17, 1977	11.70	0.0000	2
C2105	Jan. 19, 1978	-3.60	0.0000	5
C2106	March 3, 1978	0.90	0.0000	5
C2107	April 8, 1978	3.60	0.0000	5
C2108	May 10, 1978	0.50	0.0000	5
C2109	May 30, 1978	-0.30	0.0000	5
C2110	June 3, 1978	-9.90	0.0000	5
C2111	June 23, 1978	-4.70	0.0000	5
C2112	July 27, 1978	-1.60	0.0000	5
C2113	Aug. 8, 1978	-3.84	0.3600	3
C2114	Sept. 10, 1978	-0.02	0.2160	5
C2115	Oct. 13, 1978	-23.70	0.0000	5
C2116	Nov. 16, 1978	4.67	-0.2880	5
C2117	Dec. 16, 1978	-2.10	0.0000	4
C2202	Jan. 16, 1979	-1.60	0.0000	6
C2204	March 19, 1979	-0.30	0.0000	5
C2205	March 31, 1979	-1.10	0.0000	5
C2206	April 14, 1979	-2.80	0.0000	5
C2304	April 7, 1982	-16.30	0.0000	1
C2405	April 27, 1983	-1.40	0.0000	5
C2406	May 17, 1983	3.00	0.0000	5
C2502	Feb. 2, 1984	-0.70	0.0000	3
C2511	Sept. 14, 1984	10.20	0.0000	4
C9A11	July 4, 1965	0.60	0.0000	5
C9B11	July 14, 1965	2.50	0.0000	5
CAG71	Sept. 15, 1971	-0.56	-0.0288	5
CCH11	Sept. 1, 1971	0.90	0.0000	5
CCH12	Oct. 10, 1971	0.40	0.0000	5
CCHB1	Oct. 17, 1971	-3.40	0.0000	5
CCHB2	Nov. 16, 1971	-0.30	0.0000	5
CCHC1	Oct. 27, 1971	-1.70	0.0000	5
CH341	Oct. 21, 1962	1.00	0.0000	5
CH431	Feb. 19, 1964	4.90	0.0000	5
CH432	March 30, 1964	-5.40	0.0000	5
CH433	June 5, 1964	6.10	0.0000	2
CH611	July 12, 1966	-13.40	0.1008	1

TABLE A1 (continued)

Leg	Start Date	DC Shift	Drift Rate	Weight
CH612	Oct. 10, 1966	-10.90	0.0000	1
CH963	Oct. 18, 1969	4.10	0.0000	5
CH964	Nov. 2, 1969	10.30	0.0000	5
CH965	Nov. 27, 1969	-3.92	1.1232	5
CH993	May 13, 1970	-1.10	0.0000	5
CH994	June 12, 1970	-0.70	0.0000	2
CH998	Nov. 24, 1970	-0.70	0.0000	5
CM102	Aug. 17, 1961	18.00	0.0000	5
CM103	Sept. 17, 1961	0.00	0.0000	5
CMALS	July 23, 1972	0.00	0.0000	5
CMORE	May 9, 1972	4.42	-0.1152	6
CMRG1	July 23, 1972	-0.10	0.0000	7
CN003	March 2, 1971	-6.10	0.0000	8
CN004	April 1, 1971	-3.10	0.0000	5
CN005	April 25, 1971	0.10	0.0000	5
CN006	May 17, 1971	-2.60	0.0000	5
CN007	June 22, 1971	-0.60	0.0000	5
CN008	July 18, 1971	-2.90	0.0000	5
CN010	Sept. 1, 1971	-0.60	0.0000	7
CN151	Nov. 20, 1973	-4.70	0.0000	1
CN152	Dec. 14, 1973	-4.90	0.0576	4
CN153	Jan. 14, 1974	-1.40	0.0000	7
CN154	Feb. 15, 1974	0.40	0.0000	6
CN155	March 23, 1974	1.20	0.0000	5
CN156	April 22, 1974	-3.30	0.0000	9
CN157	May 22, 1974	-2.10	0.0000	5
CN158	June 1, 1974	0.58	-0.2160	2
CN159	June 24, 1974	-0.50	0.0000	5
CNCLF	March 18, 1970	0.50	0.0000	8
DATLS	Sept. 7, 1970	146.10	0.0000	5
DD671	Feb. 5, 1967	-6.18	0.1440	1
DD672	March 30, 1967	2.90	0.0000	5
DDAFZ	Aug. 17, 1970	0.00	0.0000	5
DDAMP	Oct. 10, 1965	-9.90	0.0000	5
DIS29	June 16, 1968	-12.70	0.0000	1
DIS31	Sept. 5, 1968	0.00	0.0000	5
DITRV	Aug. 26, 1970	6.80	0.0000	5
DIVCZ	Aug. 8, 1969	0.00	0.0000	5
DIVRD	July 28, 1970	0.00	0.0000	5
DMM03	Feb. 12, 1970	-1.22	0.0432	5
DMM05	Jan. 28, 1971	5.26	0.0288	5
DMM06	June 19, 1971	0.70	0.0000	2
DMM07	Dec. 29, 1971	2.26	0.0720	5
DMM09	Jan. 29, 1973	0.60	0.0000	5
DMM10	June 27, 1973	0.43	0.0288	5
DMM18	Jan. 6, 1977	-2.39	0.0000	5
DPSN1	Jan. 10, 1976	-2.40	0.0000	5
DPSN2	Feb. 9, 1976	-4.10	0.0000	2
DUT02	Aug. 11, 1970	-0.40	0.0000	7
DUT07	March 28, 1970	-1.70	0.0000	5
DUT09	June 6, 1970	0.20	0.0000	10
EE40A	Dec. 1, 1969	3.90	0.0000	5
EE41A	Jan. 29, 1970	0.90	0.0000	5
EE47A	April 20, 1971	-4.00	0.0000	5
EE54A	July 30, 1972	-3.20	0.0000	2
EE54B	Sept. 1, 1972	-2.70	0.0000	5
EE55A	Dec. 2, 1972	0.10	0.0000	5
EEL28	March 10, 1967	2.20	0.0000	1
EEL29	June 2, 1967	-1.40	0.0000	5
EEL30	Aug. 12, 1967	1.20	0.0000	5
EEL31	Nov. 15, 1967	2.40	0.0000	5
EEL32	Dec. 30, 1967	5.10	0.0000	1
EEL33	March 11, 1968	-3.60	0.0000	5
EEL34	May 28, 1968	-7.00	0.0000	5
EEL35	Aug. 12, 1968	-7.60	0.0000	5
EEL36	Oct. 18, 1968	-4.50	0.0000	5
EEL37	Jan. 10, 1969	-8.20	0.0000	5
EEL39	June 8, 1969	-5.30	0.0000	5
EEL40	Sept. 15, 1969	1.80	0.0000	5
EEL41	Dec. 20, 1969	-4.80	0.0000	5
EEL42	Feb. 28, 1970	-1.10	0.0000	5
EEL43	April 21, 1970	0.00	0.0000	5
EEL44	June 24, 1970	-2.70	0.0000	5

TABLE A1 (continued)

Leg	Start Date	DC Shift	Drift Rate	Weight
EEL45	Sept. 9, 1970	-3.30	0.0000	5
EEL47	Feb. 3, 1971	-0.80	0.0000	5
EEL48	June 28, 1971	1.40	0.0000	5
EEL49	Aug. 31, 1971	0.60	0.0000	5
EEL50	Nov. 8, 1971	0.10	0.0000	5
EEL52	Feb. 26, 1972	8.90	0.0000	5
EEL53	April 10, 1972	5.30	-0.1152	4
EEL54	June 20, 1972	-1.90	0.0000	5
EEL55	Oct. 30, 1972	1.10	0.0000	5
ENAP2	March 18, 1977	3.80	0.0000	3
EQU72	April 2, 1972	2.10	0.0000	4
FA021	Sept. 27, 1975	-1.90	0.0000	5
FA031	Oct. 2, 1975	1.10	0.0000	9
FA041	Oct. 20, 1975	0.80	0.0000	9
FA171	June 20, 1976	-14.80	0.0000	5
FA181	July 2, 1976	-14.40	0.0000	5
FA191	July 17, 1976	-0.60	0.0000	5
FA201	Aug. 10, 1976	-0.60	0.0000	5
FA211	Aug. 28, 1976	0.60	0.0000	5
FA231	Sept. 12, 1976	0.20	0.0000	5
FA251	Sept. 21, 1976	1.00	0.0000	7
FL011	Jan. 8, 1975	0.20	0.0000	5
FL012	Jan. 16, 1975	-0.80	0.0000	5
GUAY1	Feb. 9, 1978	-7.00	0.4896	1
GUAY2	March 2, 1978	-4.30	0.0000	5
GUAY3	March 8, 1978	-0.90	0.0000	5
HHD69	Aug. 16, 1969	-28.40	0.0000	5
HU117	April 27, 1969	0.00	0.0000	5
HU122	May 2, 1969	0.00	0.0000	5
HU127	May 7, 1969	6.30	0.0000	5
HU132	May 12, 1969	0.00	0.0000	5
HU140	May 20, 1969	0.00	0.0000	5
HU145	May 25, 1969	6.40	0.0000	5
HU150	May 30, 1969	27.50	0.0000	5
HU155	June 4, 1969	8.40	0.0000	5
HUD01	April 15, 1969	0.00	0.0000	5
HUD02	April 16, 1969	3.50	0.0000	5
HUD03	April 17, 1969	5.80	0.0000	5
HUD04	April 18, 1969	0.00	0.0000	5
HUD05	April 19, 1969	0.00	0.0000	5
HUD06	April 20, 1969	0.00	0.0000	5
HUD07	April 21, 1969	0.00	0.0000	5
HUD08	April 22, 1969	0.00	0.0000	5
HUD09	April 23, 1969	0.00	0.0000	5
HUD10	April 24, 1969	0.00	0.0000	5
HUD11	April 26, 1969	0.00	0.0000	5
HYPO1	March 11, 1972	0.00	0.0000	5
I0775	Oct. 31, 1975	2.60	0.0000	5
I1176	Oct. 28, 1976	-0.50	0.0000	5
I1277	Jan. 4, 1977	4.70	0.0000	5
I1377	June 25, 1977	15.99	-0.3456	5
I1578	Jan. 18, 1978	4.90	0.0000	5
I1678	April 7, 1978	3.80	0.0000	5
IIDO2	Aug. 4, 1971	1.38	-0.0576	5
IIDO3	Sept. 2, 1971	-0.20	0.0000	5
IIDO4	Sept. 30, 1971	4.75	-0.1440	5
IIDO5	Oct. 30, 1971	-6.80	0.3600	2
IND07	Aug. 14, 1976	-3.60	0.0000	5
IND08	Sept. 2, 1976	0.80	0.0000	5
IND10	Jan. 25, 1977	-12.60	0.0000	5
IND14	April 27, 1977	0.00	0.0000	5
IVK01	Jan. 14, 1978	0.80	0.0000	5
IVK1B	Feb. 20, 1978	3.92	-0.0576	5
JCH01	Aug. 3, 1969	-0.80	0.0000	5
JCH02	Aug. 28, 1969	0.80	0.0000	5
JCH03	Sept. 21, 1969	-2.30	0.0000	5
JCH04	Oct. 6, 1969	-0.80	0.0000	5
JCH05	Oct. 19, 1969	-7.10	0.0000	5
JCH06	May 26, 1971	-2.00	0.0000	5
JCH07	June 16, 1971	-0.90	0.0000	5
JCH08	July 5, 1971	-2.20	0.0000	5
JCH09	July 20, 1971	-0.60	0.0000	5
JCH10	Aug. 8, 1971	-0.10	0.0000	5

TABLE A1 (continued)

Leg	Start Date	DC Shift	Drift Rate	Weight
JCH11	Jan. 24, 1969	-0.70	0.0000	5
JCH12	May 23, 1969	-5.10	0.0000	5
JCH13	June 10, 1969	-1.90	0.0000	5
JCH15	May 10, 1970	3.90	0.0000	5
JCH16	May 28, 1970	-3.10	0.0000	5
JCH17	June 15, 1970	-4.00	0.0000	5
JCH18	Aug. 28, 1970	0.00	0.0000	5
JCH19	Sept. 14, 1970	-0.80	0.0000	5
JCH20	Sept. 29, 1970	0.00	0.0000	5
JCH21	Oct. 19, 1970	-1.60	0.0000	5
JCH22	March 7, 1971	0.00	0.0000	5
JCH23	March 25, 1972	17.40	0.0000	5
JCH24	April 10, 1972	0.00	0.0000	5
JCH25	April 21, 1972	12.20	0.0000	5
JCH26	April 25, 1972	2.10	0.0000	5
JCH27	May 14, 1972	0.10	0.0000	5
JCH28	Aug. 11, 1972	0.00	0.0000	5
JCH29	Aug. 23, 1972	0.00	0.0000	5
JCH30	Sept. 7, 1972	-3.10	0.0000	2
JCH31	Sept. 23, 1972	-7.00	0.0000	5
JCH32	Oct. 5, 1972	28.40	0.0000	5
JCH41	Sept. 6, 1973	52.50	0.0000	5
JCH44	Oct. 3, 1973	-0.20	0.0000	5
JCH48	Dec. 4, 1973	-17.15	1.2528	5
JCH49	Nov. 7, 1974	-3.10	0.0000	5
JCH50	Nov. 28, 1974	-2.40	0.0000	5
K7110	March 15, 1972	0.83	-0.1584	2
K8213	Aug. 13, 1982	0.40	0.0000	3
KE154	April 21, 1969	-0.90	0.0000	5
KE801	June 29, 1969	-4.50	0.0000	5
KE816	Dec. 4, 1969	-0.20	0.0000	5
KEA03	July 13, 1969	-1.80	0.0000	5
KEA07	Jan. 5, 1970	-1.30	0.0432	8
KEA09	May 28, 1967	-0.60	0.0000	5
KEA10	June 27, 1967	2.00	0.0000	5
KEA11	Dec. 28, 1967	-0.30	0.0000	5
KEA13	March 16, 1968	-0.30	0.0000	5
KEA14	April 16, 1968	0.40	0.0000	5
KEA15	May 23, 1968	-1.80	0.0000	9
KEA16	June 15, 1968	-0.59	0.0000	5
KEA18	July 16, 1968	-0.01	-0.0720	9
KEA19	Aug. 15, 1968	-1.52	-0.0432	8
KEA29	March 18, 1969	-0.20	0.0000	5
KEA31	Feb. 14, 1970	-1.79	0.1152	5
KEA33	April 19, 1970	-3.58	0.0576	9
KEA34	May 18, 1970	-1.10	0.0000	9
KEA35	Aug. 1, 1970	-0.60	0.0000	9
KEA37	Oct. 16, 1970	0.00	0.0000	5
KEA38	May 29, 1971	0.30	0.0000	5
KEA39	June 23, 1971	0.30	0.0000	5
KEA40	July 25, 1971	0.50	0.0000	5
KH683	July 19, 1968	3.00	0.0000	1
KK608	Jan. 23, 1972	-1.36	0.1008	4
KK609	Feb. 27, 1972	-5.38	0.2880	3
KK611	April 20, 1972	-1.50	0.0000	2
KK711	April 27, 1971	0.00	0.0000	5
KK712	May 29, 1971	0.00	0.0000	7
KK714	Sept. 2, 1971	0.70	0.0000	5
KK715	Oct. 4, 1971	0.60	0.0000	5
KK717	Dec. 19, 1971	1.10	0.0000	5
KK718	Jan. 23, 1972	-1.44	0.1008	4
KK719	Feb. 27, 1972	-5.29	0.2880	3
KK721	Nov. 8, 1972	-0.10	0.0000	5
KK722	Dec. 29, 1972	-0.40	0.0000	5
KK723	Jan. 21, 1973	0.10	0.0000	5
KK724	Feb. 20, 1973	-3.70	0.0000	5
KK725	March 6, 1973	-0.30	0.1296	5
KK726	April 3, 1973	-1.90	0.0000	5
KK727	May 1, 1973	-2.20	0.0000	4
KK728	June 2, 1973	-0.90	0.0000	5
KK72A	July 2, 1972	-1.30	0.0000	5
KK72B	Sept. 24, 1972	0.00	0.0000	5
KK730	Oct. 27, 1973	-0.60	0.0000	5

TABLE A1 (continued)

Leg	Start Date	DC Shift	Drift Rate	Weight
KK741	Jan. 10, 1974	0.00	0.0000	5
KK742	Feb. 16, 1974	-2.44	0.1584	5
KK743	April 11, 1974	-3.90	0.0000	5
KK744	May 11, 1974	-0.20	0.0000	5
KK745	May 26, 1974	-2.36	0.1728	5
KK746	June 21, 1974	-1.11	0.0144	2
KK750	July 26, 1975	0.70	0.0000	5
KK760	Oct. 10, 1976	0.40	0.0000	2
KK762	Feb. 15, 1976	6.25	0.0864	2
KK76A	Aug. 6, 1976	2.20	0.0000	1
KK76B	Sept. 5, 1976	-1.40	0.0000	2
KK771	March 17, 1977	-3.00	0.0000	4
KK772	April 8, 1977	-7.50	0.0000	6
KK773	April 21, 1977	-34.40	0.0000	1
KK774	May 13, 1977	-40.40	0.0000	4
KK775	June 8, 1977	-1.80	0.0000	2
KK805	March 6, 1973	-0.58	0.1440	5
KK806	April 3, 1973	-1.80	0.0000	5
KK816	Sept. 19, 1981	-3.90	0.0000	2
KK824	May 14, 1982	-6.90	0.0000	4
KK901	Jan. 9, 1974	-0.99	0.0000	5
KK902	Feb. 16, 1974	-1.38	0.1584	5
KK903	April 11, 1974	-4.00	0.0000	5
KK904	May 11, 1974	0.10	0.0000	5
KK905	May 26, 1974	-1.41	-0.0144	5
KK906	June 21, 1974	-1.17	0.0288	2
KK907	March 26, 1975	-3.80	0.0000	8
KKT75	Sept. 4, 1975	0.00	0.0000	5
KO20A	Jan. 18, 1975	0.20	0.0000	1
KO20B	April 28, 1975	0.30	0.0000	6
KOM15	June 20, 1973	5.20	0.0000	3
LLU01	May 15, 1962	-0.30	0.0000	5
LLU02	June 14, 1962	0.80	0.0000	5
LLU03	June 28, 1962	-6.80	0.0000	5
LLU04	July 29, 1962	4.90	0.0000	5
LLU05	Aug. 13, 1962	-0.40	0.0000	5
LLU06	Aug. 29, 1962	-10.10	0.0000	5
LLU07	Oct. 4, 1962	0.00	0.0000	5
LLU08	Oct. 18, 1962	-7.10	0.0000	5
LLU10	Dec. 2, 1962	6.70	0.0000	5
LLU13	Feb. 16, 1963	1.50	0.0000	5
LLU14	March 23, 1963	3.00	0.0000	5
LLU16	May 18, 1963	-0.10	0.0000	5
LLU18	July 7, 1963	-0.50	0.0000	5
LLU19	July 31, 1963	0.40	0.0000	5
LLU9A	Oct. 30, 1962	4.90	0.0000	5
LLU9B	Nov. 12, 1962	18.90	0.0000	5
MA680	Oct. 9, 1968	22.70	0.0000	5
MA701	April 22, 1970	2.10	0.0000	5
MA702	July 5, 1970	-4.50	0.0000	5
MA704	Sept. 23, 1970	-1.10	0.0000	5
MA705	Nov. 7, 1970	-1.70	0.0000	5
ME02T	Nov. 14, 1965	4.20	0.0000	5
ME461	Oct. 15, 1977	-2.90	0.0000	5
ME462	Oct. 19, 1977	-3.80	0.0000	5
ME463	Oct. 30, 1977	-0.50	0.0000	5
ME464	Nov. 2, 1977	-1.30	0.0000	5
ME465	Nov. 11, 1977	-0.40	0.0000	5
ME531	Feb. 13, 1980	0.00	0.0000	5
ME532	Feb. 15, 1980	-2.22	-0.2736	3
ME533	Feb. 22, 1980	-4.50	0.0000	5
ME534	Feb. 26, 1980	-6.50	0.0000	5
MET14	July 6, 1968	5.73	-0.2592	5
MET20	June 1, 1970	-0.29	-0.0144	4
MET45	Aug. 1, 1977	-4.80	0.0000	5
MMAP_	Feb. 27, 1963	0.00	0.0000	5
MMN01	Aug. 26, 1960	-1.30	0.0000	5
MMN02	Sept. 17, 1960	-5.10	0.0000	5
MMN03	Oct. 8, 1960	-5.00	0.0000	5
MMN04	Oct. 19, 1960	2.10	0.0000	5
MMN05	Nov. 18, 1960	2.20	0.0000	5
MMN06	Dec. 10, 1960	-0.70	0.0000	5
MMTR1	Dec. 17, 1968	-5.80	0.0000	5

TABLE A1 (continued)

Leg	Start Date	DC Shift	Drift Rate	Weight
OO110	April 12, 1962	2.50	0.0000	5
OO111	April 17, 1962	3.80	0.0000	5
OO611	Nov. 8, 1961	0.90	0.0000	5
OO612	Jan. 29, 1962	1.60	0.0000	5
OO613	Feb. 13, 1962	-6.20	0.0000	5
OO614	Feb. 22, 1962	0.00	0.0000	5
OO615	Feb. 23, 1962	0.00	0.0000	5
OO616	Feb. 25, 1962	7.10	0.0000	5
OO617	Feb. 27, 1962	0.30	0.0000	5
OO618	Feb. 28, 1962	3.50	0.0000	5
OO619	March 11, 1962	-3.00	0.0000	5
OO621	Nov. 1, 1962	0.70	0.0000	2
OO622	Nov. 30, 1962	-0.20	0.0000	5
OO623	Dec. 10, 1962	-0.10	0.0000	5
OO624	April 8, 1963	-2.80	0.0000	5
OOSSD	May 15, 1967	5.90	0.0000	5
OOSSE	May 28, 1967	1.80	0.0000	5
OOSSE	June 13, 1967	3.90	0.0000	5
OOSSE	June 28, 1967	-5.20	0.0000	5
OOSSE	July 21, 1967	0.80	0.0000	5
OOSSE	Aug. 29, 1967	23.50	0.0000	5
OPFZ1	Aug. 12, 1969	1.45	-0.0864	6
OPR41	June 16, 1968	-11.80	0.0000	1
OPR43	Sept. 5, 1968	0.00	0.0000	5
OR476	Oct. 11, 1967	0.00	0.0000	5
P6202	April 4, 1962	0.00	0.0000	5
P6702	Oct. 11, 1967	-1.10	0.0000	5
P7004	Sept. 24, 1970	15.00	0.0000	5
P7008	Jan. 17, 1970	-1.20	0.0000	5
P7101	April 16, 1971	0.00	0.0000	5
P7103	April 5, 1971	-5.29	0.0576	5
P7108	Aug. 25, 1971	3.20	0.0000	7
P7201	March 7, 1972	-12.30	-0.0144	1
P7301	Feb. 13, 1973	-0.70	0.0000	5
P7302	March 8, 1973	-0.30	0.0000	5
P7303	April 5, 1973	-4.68	0.0288	5
P7304	May 17, 1973	-0.20	0.0000	5
PEGA1	Jan. 10, 1972	0.00	0.0000	5
PIO64	Feb. 26, 1964	0.60	0.0000	3
PPI17	Feb. 16, 1963	0.00	0.0000	5
PPI21	May 5, 1963	0.00	0.0000	5
PPI28	March 26, 1965	0.00	0.0000	5
PPI5B	May 2, 1961	0.00	0.0000	5
PPI5C	May 1, 1961	0.00	0.0000	5
PPI6E	May 10, 1963	0.00	0.0000	5
PPI6W	Sept. 15, 1961	0.00	0.0000	5
PPI7E	Sept. 9, 1961	11.70	0.0000	5
PZGSC	May 23, 1972	1.90	0.0000	4
SH375	March 29, 1975	-9.30	0.0000	1
SH475	April 18, 1975	-9.90	0.0000	1
SH977	Aug. 17, 1977	6.17	0.2016	5
SR721	March 18, 1972	-2.20	0.0000	1
SS005	Dec. 3, 1964	-2.00	0.0000	5
SS006	Jan. 15, 1965	-2.10	0.0000	5
SS007	Feb. 8, 1965	0.10	0.0000	5
SS008	March 13, 1965	-3.95	-0.1728	5
SS009	April 8, 1965	-6.00	0.0000	5
SS010	May 11, 1965	-2.60	0.0000	5
SS011	June 1, 1965	0.90	0.0000	5
SS012	June 25, 1965	0.00	0.0000	5
SS013	July 28, 1965	-3.00	0.0000	5
SS014	Aug. 31, 1965	4.50	0.0000	5
SS020	Nov. 10, 1964	-12.20	0.0000	5
SS12A	Aug. 20, 1965	-9.10	0.0000	5
SV370	March 17, 1970	-9.12	0.0432	10
SV970	Aug. 19, 1970	-0.40	0.0000	9
TAG70	July 9, 1970	3.61	-0.2880	5
TAG71	April 8, 1971	-3.60	0.0000	5
TT20B	Nov. 21, 1968	-10.80	0.0000	5
TTG4A	Jan. 5, 1965	0.00	0.0000	5
TTP4A	Jan. 1, 1974	-0.10	0.0000	5
UMPPI	July 21, 1965	4.40	0.0000	3
USGS1	May 27, 1971	-6.00	0.0000	1

TABLE A1 (continued)

Leg	Start Date	DC Shift	Drift Rate	Weight
USGS2	June 21, 1971	-0.40	0.0000	5
USGS3	July 17, 1971	0.00	0.0000	5
USGS4	Aug. 18, 1971	-1.10	0.0144	2
USGS5	Oct. 30, 1971	-2.56	0.1008	1
USGS6	Nov. 24, 1971	-2.62	0.2304	5
V1704	Jan. 12, 1961	3.60	0.0000	5
V1705	Feb. 18, 1961	2.80	0.0000	5
V1708	April 1, 1961	-3.70	0.0000	5
V1710	May 4, 1961	-15.90	0.0000	5
V1711	May 22, 1961	16.40	0.0000	5
V1712	June 27, 1961	12.20	0.0000	5
V1713	July 19, 1961	3.90	0.0000	5
V1717	Sept. 23, 1961	-2.20	0.0000	5
V1802	Dec. 6, 1961	-0.10	0.0000	5
V1803	Dec. 27, 1961	2.60	0.0000	5
V1804	Jan. 21, 1962	5.80	0.0000	5
V1805	Feb. 11, 1962	0.90	0.0000	5
V1806	Feb. 23, 1962	2.90	0.0000	5
V1807	March 14, 1962	-4.20	0.0000	5
V1808	April 6, 1962	3.10	0.0000	5
V1809	May 9, 1962	-0.80	0.0000	5
V1810	June 3, 1962	-2.10	0.0000	5
V1811	June 22, 1962	33.80	0.0000	5
V1812	July 14, 1962	-4.40	0.0000	5
V1813	Aug. 5, 1962	-5.50	0.0000	5
V1815	Sept. 19, 1962	0.60	0.0000	5
V1816	Oct. 16, 1962	12.10	0.0000	5
V1817	Oct. 28, 1962	17.19	0.0576	5
V1818	Nov. 14, 1962	1.10	0.0000	5
V1819	Nov. 25, 1962	2.70	0.0000	5
V1903	March 15, 1963	4.70	0.0000	5
V1904	March 31, 1963	0.30	0.0000	5
V1905	April 14, 1963	-0.30	0.0000	5
V1906	May 10, 1963	3.80	0.0000	5
V1907	May 21, 1963	-0.60	0.0000	5
V1908	June 22, 1963	2.90	0.0000	5
V1909	July 11, 1963	1.20	0.0000	5
V1910	Aug. 8, 1963	1.70	0.0000	5
V1911	Aug. 28, 1963	1.00	0.0000	5
V1912	Sept. 20, 1963	1.60	0.0000	5
V1913	Nov. 15, 1963	7.20	0.0000	5
V2002	March 2, 1964	-10.79	2.2320	5
V2003	March 17, 1964	0.00	0.0000	5
V2004	April 20, 1964	-7.50	0.0000	5
V2005	May 7, 1964	3.20	0.0000	5
V2006	May 27, 1964	0.50	0.0000	5
V2007	July 3, 1964	5.00	0.0000	5
V2008	July 30, 1964	1.60	0.0000	5
V2009	Aug. 23, 1964	-3.10	0.0000	5
V2010	Sept. 21, 1964	-14.50	0.0000	5
V2011	Oct. 14, 1964	-30.60	0.0000	5
V2012	Nov. 11, 1964	-13.10	0.0000	5
V2013	Dec. 5, 1964	-14.10	0.0000	5
V2101	Feb. 11, 1965	1.40	0.0000	5
V2103	Feb. 28, 1965	-6.30	0.0000	5
V2104	March 14, 1965	0.80	0.0000	5
V2105	April 14, 1965	-2.50	0.0000	5
V2106	May 7, 1965	-4.20	0.0000	5
V2107	June 15, 1965	-8.70	0.0000	5
V2108	July 8, 1965	-3.80	0.0000	5
V2110	Aug. 8, 1965	-3.00	0.0000	5
V2111	Sept. 6, 1965	3.70	0.0000	5
V2112	Sept. 16, 1965	14.30	0.0000	5
V2113	Oct. 11, 1965	-2.98	0.1872	5
V2114	Nov. 14, 1965	1.72	-0.0144	4
V21A9	Aug. 1, 1965	0.00	0.0000	5
V21B9	Aug. 3, 1965	-10.30	0.0000	5
V2201	Jan. 10, 1966	-1.54	0.1584	5
V2202	Jan. 30, 1966	0.85	0.0144	5
V2203	Feb. 18, 1966	3.70	0.0000	5
V2204	March 16, 1966	1.50	0.0000	5
V2205	April 16, 1966	2.30	0.0000	5
V2206	April 26, 1966	2.40	0.0000	5

TABLE A1 (continued)

Lég	Start Date	DC Shift	Drift Rate	Weight
V2207	May 25, 1966	-3.90	0.0000	5
V2301	July 27, 1966	6.60	0.0000	5
V2302	Aug. 8, 1966	-3.80	0.0000	5
V2303	Aug. 27, 1966	0.70	0.0000	3
V2304	Sept. 17, 1966	1.05	-0.1008	5
V2305	Oct. 15, 1966	-0.60	0.0000	5
V2306	Nov. 6, 1966	2.00	0.0000	3
V2307	Dec. 8, 1966	5.30	0.0000	5
V2401	Jan. 16, 1967	0.35	-0.0144	4
V2402	Jan. 31, 1967	-2.30	0.0000	5
V2403	Feb. 21, 1967	0.24	-0.0432	5
V2404	March 27, 1967	-1.40	0.0000	5
V2405	April 25, 1967	-0.84	-0.1296	5
V2406	May 31, 1967	4.20	0.0000	5
V2407	June 16, 1967	-9.61	0.6912	5
V2408	July 18, 1967	-2.00	0.0000	5
V2409	Aug. 13, 1967	2.50	0.0000	5
V2410	Aug. 22, 1967	-15.10	0.0000	5
V2411	Sept. 21, 1967	3.60	0.0000	5
V2412	Oct. 16, 1967	-4.10	0.0000	5
V2413	Nov. 17, 1967	5.68	-0.1728	5
V2501	Jan. 5, 1968	-5.29	-0.0432	6
V2502	Feb. 8, 1968	-2.27	0.2304	5
V2503	March 11, 1968	3.38	0.5328	5
V2504	April 5, 1968	11.88	-1.2240	5
V2604	Oct. 26, 1968	-0.60	0.0000	8
V2605	Nov. 29, 1968	-1.80	0.0000	9
V2606	Jan. 2, 1969	-1.90	0.0000	7
V2607	Feb. 3, 1969	-22.30	0.0000	4
V2608	March 5, 1969	0.98	-0.0144	5
V2609	April 11, 1969	2.20	0.0000	4
V2610	May 12, 1969	16.70	0.0000	5
V2701	May 29, 1969	-6.90	0.0000	5
V2702	June 20, 1969	-0.60	0.0000	5
V2703	July 19, 1969	1.00	0.0000	5
V2704	Aug. 10, 1969	3.51	-0.4176	7
V2705	Sept. 12, 1969	-1.20	0.0000	5
V2706	Sept. 20, 1969	0.30	0.0000	5
V2707	Oct. 19, 1969	-3.00	0.0000	5
V2708	Nov. 21, 1969	1.50	0.0000	5
V2709	Dec. 3, 1969	1.13	-0.1440	5
V2710	Jan. 2, 1970	-1.34	-0.1584	5
V2711	Feb. 6, 1970	-2.40	0.0000	5
V2712	Feb. 13, 1970	-0.40	0.0000	5
V2713	March 15, 1970	0.48	0.0432	5
V2714	April 13, 1970	0.50	0.0000	5
V2801	June 25, 1970	1.50	0.0000	5
V2802	July 18, 1970	-2.00	0.0000	5
V2803	Aug. 6, 1970	-0.86	0.0288	5
V2804	Sept. 10, 1970	1.60	0.0000	5
V2805	Oct. 11, 1970	0.00	0.0000	5
V2806	Nov. 6, 1970	2.70	0.0000	5
V2807	Nov. 24, 1970	-2.76	0.1008	5
V2808	Dec. 28, 1970	0.00	0.0000	5
V2809	Jan. 9, 1971	0.10	0.0000	4
V2810	Feb. 5, 1971	-0.50	0.0000	5
V2811	March 12, 1971	0.30	0.0000	4
V2812	April 14, 1971	0.20	0.0000	5
V2813	April 21, 1971	1.20	0.0000	5
V2814	May 20, 1971	3.00	0.0000	5
V2815	June 22, 1971	2.60	0.0000	5
V2816	July 22, 1971	1.80	0.0000	5
V2817	Aug. 13, 1971	6.02	0.1008	5
V2818	Sept. 14, 1971	2.80	0.0000	5
V2819	Oct. 15, 1971	-9.20	0.0000	5
V2901	Nov. 18, 1971	-3.80	0.0000	5
V2902	Dec. 18, 1971	-2.80	0.0000	5
V2903	Jan. 20, 1972	1.20	0.0000	5
V2904	Feb. 18, 1972	0.70	0.0000	5
V2905	March 21, 1972	-35.10	0.0000	5
V2906	April 21, 1972	-1.10	0.0000	5
V2907	May 21, 1972	-2.60	0.0000	5
V2908	June 15, 1972	1.85	0.0864	5

TABLE A1 (continued)

Leg	Start Date	DC Shift	Drift Rate	Weight
V2909	July 14, 1972	1.07	0.0000	5
V2910	Aug. 11, 1972	0.29	-0.0720	5
V2911	Sept. 12, 1972	0.30	0.0000	5
V2912	Oct. 10, 1972	0.70	0.0000	5
V3001	Nov. 22, 1972	1.78	-0.2016	5
V3002	Dec. 8, 1972	1.54	-0.1584	5
V3003	Jan. 4, 1973	0.00	0.0000	5
V3004	Feb. 2, 1973	0.30	0.0000	5
V3005	March 3, 1973	-2.00	0.0000	5
V3006	March 31, 1973	-0.81	-0.0288	4
V3007	April 28, 1973	-1.42	-0.2736	3
V3008	May 26, 1973	-1.00	0.0000	5
V3009	June 23, 1973	-0.10	0.0000	6
V3010	July 26, 1973	-0.30	0.0000	7
V3011	Aug. 29, 1973	-3.42	0.0720	9
V3012	Oct. 5, 1973	-0.10	0.0000	5
V3013	Nov. 1, 1973	1.00	0.0000	3
V3014	Dec. 4, 1973	3.22	0.2304	5
V3101	Jan. 2, 1974	-0.40	0.0000	5
V3102	Feb. 2, 1974	0.60	0.0000	5
V3103	March 7, 1974	-6.53	0.1584	5
V3104	April 6, 1974	-0.70	0.0000	7
V3105	May 8, 1974	-1.80	0.0000	5
V3106	June 3, 1974	0.66	0.0864	5
V3107	July 5, 1974	0.60	0.0000	6
V3108	Aug. 6, 1974	-1.80	0.0000	5
V3201	Oct. 17, 1974	0.20	0.0000	5
V3202	Nov. 5, 1974	-0.20	0.0000	5
V3203	Nov. 21, 1974	1.20	0.0000	4
V3204	Dec. 22, 1974	3.53	-0.0144	5
V3205	Jan. 19, 1975	4.03	-0.2880	5
V3206	Feb. 18, 1975	0.10	0.0000	4
V3207	March 23, 1975	0.20	0.0000	6
V3208	April 24, 1975	0.20	0.0000	5
V3209	May 12, 1975	0.45	-0.5328	5
V3210	May 31, 1975	1.00	0.0000	5
V3211	July 1, 1975	0.90	0.0000	5
V3212	July 18, 1975	-5.80	0.0000	5
V3213	Aug. 19, 1975	-0.50	0.0000	5
V3214	Sept. 18, 1975	1.20	0.0000	1
V3215	Oct. 18, 1975	-0.50	0.0000	5
V3301	Nov. 17, 1975	-0.70	0.0000	5
V3303	Jan. 20, 1976	0.70	0.0000	5
V3304	Feb. 23, 1976	-0.50	0.0000	5
V3305	March 18, 1976	-2.70	0.0000	5
V3306	April 19, 1976	0.80	0.0000	5
V3307	May 16, 1976	-2.50	0.0000	5
V3308	June 15, 1976	-1.80	0.0000	5
V3309	July 25, 1976	1.40	0.0000	5
V3310	Aug. 27, 1976	-0.10	0.0000	5
V3311	Sept. 25, 1976	-1.30	0.0000	5
V3312	Nov. 27, 1976	-1.80	0.0000	5
V3313	Dec. 20, 1976	0.50	0.0000	5
V3314	Jan. 21, 1977	5.30	0.0000	5
V3401	Feb. 22, 1977	6.50	0.0000	5
V3402	March 25, 1977	11.30	0.0000	2
V3403	April 25, 1977	7.50	0.0000	5
V3404	May 28, 1977	4.00	0.0000	2
V3405	June 28, 1977	2.50	0.0000	5
V3406	Aug. 1, 1977	10.50	0.0000	5
V3407	Aug. 30, 1977	9.10	0.0000	5
V3408	Oct. 2, 1977	4.40	0.0000	5
V3409	Nov. 2, 1977	3.50	0.0000	4
V3410	Dec. 10, 1977	0.10	0.0000	5
V3411	Jan. 4, 1978	3.90	0.0000	5
V3501	Feb. 18, 1978	-0.90	0.0000	5
V3502	March 9, 1978	2.39	-0.0720	5
V3503	April 9, 1978	-4.10	0.0000	5
V3504	May 25, 1978	2.50	0.0000	5
V3505	June 4, 1978	1.00	0.0000	5
V3506	July 6, 1978	3.00	0.0000	5
V3602	Aug. 14, 1979	10.70	0.0000	5

TABLE A1 (continued)

Leg	Start Date	DC Shift	Drift Rate	Weight
V3603	Oct. 10, 1979	-0.97	-0.0144	1
V3604	Nov. 12, 1979	-3.90	0.0000	5
V3605	Dec. 5, 1979	3.20	0.0000	5
V3606	Dec. 24, 1979	20.60	0.0000	5
V3607	Jan. 13, 1980	6.90	0.0000	5
V3608	Feb. 11, 1980	3.80	0.0000	5
V3609	March 7, 1980	4.50	0.0000	5
V3610	April 8, 1980	9.20	0.0000	5
V3611	May 2, 1980	2.40	0.0000	5
V3612	May 24, 1980	0.47	-0.0288	8
V3613	June 28, 1980	-0.70	0.0000	3
V3614	Aug. 2, 1980	5.46	-0.1440	5
V3616	Sept. 12, 1980	2.70	0.0000	5
V3617	Oct. 15, 1980	2.20	0.0000	5
V3618	Nov. 17, 1980	0.30	0.0000	5
V3619	Dec. 20, 1980	-1.39	0.4176	5
V3620	Jan. 19, 1981	10.10	0.0000	5
V3621	Feb. 12, 1981	3.80	0.0000	5
VA791	Sept. 25, 1979	-1.50	0.0000	5
VA792	Sept. 30, 1979	0.00	0.0000	5
VA793	Oct. 4, 1979	1.00	0.0000	5
VA794	Oct. 9, 1979	-2.00	0.0000	5
VA795	Oct. 13, 1979	-1.10	0.0000	5
VA796	Oct. 15, 1979	-0.40	0.0000	5
VIT43	March 11, 1968	0.60	0.0000	2
VIT49	Nov. 14, 1970	-1.31	0.1440	5
VIT51	Jan. 26, 1972	0.40	0.0000	1
VIT72	Sept. 13, 1972	0.00	0.0000	5
WE752	Dec. 6, 1975	2.04	-0.8640	5
WE753	Dec. 17, 1975	-2.63	-0.0864	5
WWHC1	Oct. 23, 1968	0.00	0.0000	5
WWHC2	Oct. 28, 1968	0.00	0.0000	5
WWHC5	Nov. 30, 1968	0.00	0.0000	5
YQ67A	April 18, 1967	-0.80	0.0000	5
YQ67G	Aug. 1, 1967	-2.33	0.1440	5
YQ67L	July 31, 1967	1.80	0.0000	5
YQ68S	Sept. 7, 1968	0.00	0.0000	5
YQ69A	April 2, 1969	11.70	0.0000	5
YQ69F	Feb. 14, 1969	-6.50	0.0000	5
YQ703	Aug. 28, 1970	23.70	0.0000	5
YQ704	Sept. 15, 1970	41.60	0.0000	5
YQ705	Oct. 11, 1970	11.00	0.0000	5
YQ710	April 14, 1972	-0.10	0.0000	5
YQ712	Aug. 29, 1971	0.00	0.0000	5
YQ716	Jan. 5, 1972	-0.20	0.0000	5
YQ718	Feb. 26, 1972	3.14	0.0432	1
YQ719	March 15, 1972	-0.90	0.0000	3
YQ730	April 22, 1974	1.90	0.0000	5
YQ732	Sept. 20, 1973	0.10	0.0000	5
YQ735	Jan. 4, 1974	-0.90	0.0000	5
YQ736	Jan. 19, 1974	0.42	-0.1296	5
YQ737	Feb. 17, 1974	-3.66	0.1152	6
YQ738	March 19, 1974	-4.79	0.3024	5
YQ739	March 30, 1974	-0.90	0.0000	5
YYAQ6	Jan. 6, 1972	0.00	0.0000	5
YYAQ7	Jan. 24, 1972	0.00	0.0000	5

Acknowledgments. This work was supported by grants TO-204 scope I and TO-0132 scope B from the Office of Naval Research. We thank J. R. Cochran, W. F. Haxby, D. G. Martinson, R. H. Rapp, and W. H. F. Smith for helpful discussions and comments. Lamont-Doherty Geological Observatory contribution 4221.

REFERENCES

- Akima, H., Interpolation and smooth curve fitting based on local procedures, *Commun. ACM*, 15, 914-918, 1972.
 Bell, R., and A. B. Watts, Evaluation of the BGM-3 sea gravimeter

- system on board R/V *Conrad*, *Geophysics*, 51, 1480-1493, 1986.
- Brammer, R. F., and R. V. Sailor, Preliminary estimates of the resolution capability of the Seasat radar altimetry, *Geophys. Res. Lett.*, 7, 193-196, 1980.
- Briggs, I. C., Machine contouring using minimum curvature, *Geophysics*, 39, 39-48, 1974.
- Cheney, R. E., and J. G. Marsh, Seasat altimeter observations of dynamic topography in the Gulf Stream region, *J. Geophys. Res.*, 86, 473-483, 1981.
- Dehlinger, P., *Marine Gravity*, Elsevier, New York, 1978.
- Graf, A., and R. Schulze, Improvements on the sea gravimeter Gss2, *J. Geophys. Res.*, 66, 1813-1821, 1961.
- Kamer, G. D., and A. B. Watts, Gravity anomalies and flexure of the lithosphere at mountain ranges, *J. Geophys. Res.*, 88, 10,449-10,477, 1983.
- Lacoste, L. J. B., Surface ship gravity measurements on the Texas A&M College ship *Hidalgo*, *Geophysics*, 24, 309-322, 1959.
- Ligon, J. M., NAVSTAR-GPS at sea results, *Mar. Geod.*, 9, 227-261, 1985.
- Marsh, J. G., F. J. Learch, and R. G. Williamson, Precision geodesy and geodynamics using Starlette laser ranging, *J. Geophys. Res.*, 90, 9335-9345, 1985.
- Neuman, L.D. and M. Talwani, Accelerations and errors in gravity measurements on surface ships, *J. Geophys. Res.*, 77, 4330-4338, 1972.
- Prince, R. A., and D. W. Forsyth, A simple objective method for minimizing crossover errors in marine gravity data, *Geophysics*, 44, 1079-1083, 1984.
- Rapp, R. H., The Earth's gravity field to degree and order 180 using Seasat altimetry data, terrestrial data and other data, Ohio State Univ., Dep. of Geod. Sci., Columbus, Rep. 322, 53 pp., 1981.
- Swain, C. J., A FORTRAN IV program for interpolating irregularly spaced data using the difference equations for minimum curvature, *Comput. Geosci.*, 1, 231-240, 1976.
- Talwani, M., Some recent developments in gravity measurements aboard surface ships, in: *Gravity Anomalies: Unsurveyed Areas*, *Geophys. Monogr.*, 9, edited by H. Orlin, pp. 31-47, AGU, Washington, D. C., 1966.
- Talwani, M. Gravity, in *The Sea*, vol. 4, part 1, edited by A. Maxwell, pp. 251-297, John Wiley, New York, 1971.
- Watts, A. B., G. D. Kamer, P. Wessel, and J. Hastings, Global gravity data bank system, *Tech. Rep. 4, CU-1-85*, Office of Nav. Res., Washington, D. C., 1985.
- Wunsch, C., and E. M. Gaposchkin, On using satellite altimetry to determine the general circulation of the oceans with application to geoid improvement, *Rev. Geophys.*, 18, 725-745, 1980.
- Zlotnicki, V., On the accuracy of gravimetric geoids and the recovery of oceanographic signals from altimetry, *Mar. Geod.*, 8, 129-157, 1984.

A. B. Watts and P. Wessel, Lamont-Doherty Geological Observatory and Department of Geological Sciences, Columbia University, Palisades, NY 10964.

(Received May 1, 1987;
accepted July 29, 1987.)